

7-5-2012

# Channel rehabilitation to increase aquatic habitat and reestablish floodplain connectivity on the Upper Gila River

Eric Scherff

Follow this and additional works at: [https://digitalrepository.unm.edu/wr\\_sp](https://digitalrepository.unm.edu/wr_sp)

---

## Recommended Citation

Scherff, Eric. "Channel rehabilitation to increase aquatic habitat and reestablish floodplain connectivity on the Upper Gila River." (2012). [https://digitalrepository.unm.edu/wr\\_sp/56](https://digitalrepository.unm.edu/wr_sp/56)

This Technical Report is brought to you for free and open access by the Water Resources at UNM Digital Repository. It has been accepted for inclusion in Water Resources Professional Project Reports by an authorized administrator of UNM Digital Repository. For more information, please contact [disc@unm.edu](mailto:disc@unm.edu).

# **Channel rehabilitation to increase aquatic habitat and reestablish floodplain connectivity on the Upper Gila River**

**by**

**Eric J. Scherff**

Committee  
Dr. Cliff Dahm, Chair  
Dr. Vicenç Acuña  
Dr. Julie Coonrod

A Professional Project Report Submitted in Partial Fulfillment of the Requirements  
for the Degree of  
**Master of Water Resources**  
Hydroscience Concentration  
Water Resources Program  
The University of New Mexico  
Albuquerque, New Mexico  
December 2011

## Committee Approval

The Master of Water Resources Professional Project Report of **Eric J. Scherff**, entitled **Channel rehabilitation to increase aquatic habitat and reestablish floodplain connectivity on the Upper Gila River**, is approved by the committee:

---

Chair

---

Date

---

---

---

---

---

---

# Table of Contents

List of Tables .....	iii
List of Figures.....	iv
Acknowledgements.....	vi
ABSTRACT.....	1
INTRODUCTION .....	2
METHODS .....	11
Study site.....	11
Site history .....	14
Geospatial data.....	15
High-resolution laser survey .....	15
Processing LIDAR data .....	16
Parsing.....	16
Merging and aligning.....	17
Georeferencing.....	19
Bare-earth point classification .....	21
Bathymetry.....	23
Channel survey and data processing.....	23
Bathymetry interpolation .....	23
Digital Terrain Model .....	24
Stream geometry and alternate channel configurations .....	25
Hydraulic model.....	26
Software .....	26
Boundary conditions .....	27
Choice and characterization of modeled flows .....	28
Roughness coefficient.....	29
Habitat availability and floodplain connectivity assessment .....	30
RESULTS .....	31
Site history .....	31
Geospatial data processing.....	35

High-resolution laser survey and data processing. ....	35
Merging and aligning.....	36
Georeferencing.....	36
Elevation model and choice of alternate channel configurations .....	36
Hydraulic model.....	41
Roughness coefficient.....	41
Simulation of flooded area.....	41
Simulation of water volume.....	45
Simulation of inundation patterns and floodplain connectivity .....	48
Characterization of flows .....	54
DISCUSSION .....	55
CONCLUSIONS.....	60
REFERENCES .....	62
APPENDIX.....	79
Appendix 1.....	79

## List of Tables

Table I. References to channel modification events from handwritten notes on Discharge Measurement Notes and from the Station Description (USGS, 2010c.).....	32
Table II. Roughness coefficients for hydraulic model.....	41

## List of Figures

Figure 1. Study area location. ....	12
Figure 2. Daily mean discharge statistics for the period 1928-2010 at streamflow gaging station 09430500, Gila River near Gila .....	13
Figure 3. Aerial photos of the upstream end of the study site taken in 1950 and 1965.....	33
Figure 4. Aerial photo of study site dated October 1966.....	34
Figure 5. 1972 photo at the upstream end of the study site .....	35
Figure 6. TIN surface representing bare-earth at site viewed in ArcScene .....	37
Figure 7. Plan view of surface model of the study site.....	39
Figure 8. TIN surface showing location of overflow channel proposed for site .....	40
Figure 9. Total flooded area within study reach based on simulations in HEC-RAS and GIS analysis .....	43
Figure 10. Absolute difference in flooded area and percent difference in flooded area between restored and existing channel and floodplain geometry based on simulations in HEC-RAS and GIS analysis.....	44
Figure 11. Mapped hydraulic model results for the flow of 500 cms with the restored channel plan. ....	45
Figure 12. Total flooded volume within study reach based on simulations in HEC-RAS and GIS analysis.....	47
Figure 13. Absolute difference in flooded volume and percent difference in flooded volume between restored and existing channel and floodplain geometry based on simulations in HEC-RAS and GIS analysis. ....	48
Figure 14. Water surface formed by a backwater in proposed overflow channel .....	49

Figure 15. Simulated water depths illustrating flooded area and differences in inundation patterns ..... 51

Figure 16. Plan view of study site showing maximum width of flooded area for the existing configuration and the restored configuration at 10 cms of discharge and 100 cms of discharge..... 53

Figure 17. Percent exceedance analysis of daily mean flows by season for the period 1928-2010 at streamflow gaging station 09430500, Gila River near Gila ..... 55

## **Acknowledgements**

I am grateful to many individuals and organizations that helped me complete this project. My committee allowed me to explore the questions I found most intriguing while also pointing out the most salient parts of the system. Professor Cliff Dahm shared his knowledge about the environmental backdrop of stream ecology in this semi-arid region, which allowed me to better appreciate and describe my findings. He also impressed upon me that science has a key role to inform the decisions society makes to manage the environment. Dr. Julie Coonrod showed unfailing confidence in my abilities as she listened to my ideas. Her refreshing optimism reminded me at difficult points in the process that there must be a way to move forward and that I would find it. Additionally, Dr. Coonrod helped develop a GIS technique to create the detailed river terrain model that was a central part of this study. My committee would not have been complete without the vision and resolve of Dr. Vicenç Acuña. I thank him for introducing me to the Gila, and for pointing out connections between physical form and processes that increased my appreciation for the landscape immensely. He made it clear that my research could tell a story about this stream reach, and his patience and encouragement were phenomenal.

This project was completed with generous technical assistance from the Lidar Lab of the University of New Mexico. Lab Director Dr. Tim Wawrzyniec made this possible, and Research Scientist Jed Frechette shared his in-depth knowledge of geospatial data techniques and unrelenting problem-solving ability to resolve several impasses in the development of spatial models. Financial assistance from T & E, Inc. supported this research. I am also grateful to the Wootten family for allowing me to use their cabin to store scanning equipment when difficulties

in site access arose unexpectedly. The Nature Conservancy (TNC) owns the unique property on which this research site is located, and kindly granted permission to carry out the study. The aid of TNC Southwest NM Field Representative Martha Schumann was much appreciated.

Many others contributed to this project. From the USGS, I would like to thank Scott Christenson for assistance with geospatial data and perspective on the research process, George Sieber and Tino Quintana for historical and hydrologic background about the study site, Anne Tillery for guidance on hydraulic model development, and Gerald Bawden for providing state-of-the-art bare-earth point classification of our LIDAR data. Dr. Venkatesh Merwade gave technical support in the use of the GIS bathymetry tool that he developed. The geomorphology of the research site occasionally became an obsession, and this was satisfied through discussion with Dr. Grant Meyer, Ellen Soles, and David Menzie. Dr. John Hawley shared bibliographic information related to the region, including one of the first written accounts from an early explorer in the Gila. Kelly Isaacson communicated her experience with processing stream geometry data in HEC-GeoRAS. Dr. Mark Stone provided an excellent introduction to several topics on stream restoration in his seminar course, and this provided an important perspective on my work. I would also like to thank Professor Bruce Thomson, Director of the Water Resources Program, for encouraging me, expecting excellence, and offering to help in any way possible.

The support and influence of my family has been tremendously important in the completion of this project. My wife encouraged me to pursue my dream of studying water resources, and has done everything she can to help me realize this, including more than her fair share of just

about everything. My sister has shared her perspective as an environmental professional, and has reminded me more than once that I will finish this undertaking—and that it will be great! My parents have always been pleased that I find my work interesting, and for them this is the most important thing.

## ABSTRACT

Stream restoration is an opportunity to recover a substantial amount of lost ecosystem structure and function. This may be particularly beneficial for perennial streams in semi-arid regions because of the striking differences in productivity and biodiversity between the riparian corridor and surrounding uplands. We develop a plan to restore floodplain connectivity along a channelized reach of the unregulated Upper Gila River in southwestern New Mexico, and evaluate its potential to provide additional aquatic habitat. To identify the extent of historical channelization, primary and secondary documents are examined. Signs of current geomorphic processes are also considered to formulate a restoration design. A high-resolution elevation model of the channel and floodplain is built from Light Detection and Ranging (LIDAR) and channel survey data, and an additional elevation model is created that includes the restoration plan. The plan consists of a new overflow channel in the disconnected floodplain, and is evaluated using a hydraulic model of open channel flow built with stream geometry information from the georeferenced elevation model. Flow levels for the study are chosen and characterized based on the 83-year record of daily mean discharge measured at the gaging station immediately upstream of the study site. The hydraulic simulation estimates for total area, total volume, and patterns of inundation in the study reach are used to evaluate the change in aquatic habitat availability and floodplain connectivity for the restoration plan. Results show that the reconfigured channel pattern would provide unique backwater habitat in the reach, and it also would increase total flooded area and floodplain connectivity throughout the entire range of modeled discharges.

## INTRODUCTION

Degradation of river floodplains has been happening throughout the world with increased human settlement (Tockner and Stanford, 2002). Humans have caused this impairment largely by physical changes to riparian areas, including channel modification, dam construction, and flow regulation (Brookes, 1988; Ward and Stanford, 1995; Graf, 2001; Lloyd *et al.*, 2003). The widespread effects such changes have had on landscapes and ecosystems are apparent in the history of Asia, Europe, Australia, New Zealand, and North America (Brookes *et al.*, 1983; Xu, 1993; Maddock, 1999; Kingsford, 2000; Ward *et al.*, 2001; Wohl, 2005; Nakano and Nakamura, 2006; Reid *et al.*, 2008). For example, the expansive alluvial plain of the Lower Yellow River, considered to be the cradle of Chinese civilization, already had a system of artificial levees in 221 B.C. (Xu, 1993). Dikes were built along the Rhine River and its distributaries in the Netherlands between 1050 and 1350 AD as protection against frequent floods and to increase the land available for agricultural production (Van Urk and Smit, 1989; Hesselink *et al.*, 2003). The settlement of Australia by Europeans brought river management practices to this continent more recently, and studies show that in only 200 years considerable change has taken place along its waterways. This includes an estimated 50% reduction in flooded area of floodplain wetlands with subsequent declines found in the health of aquatic vegetation, water-birds, fish and invertebrate populations (Kingsford, 2000).

Perhaps the most rapid and extensive execution of floodplain management has been in the USA, where it has followed westward expansion of the population. Levees were built on the Mississippi River beginning in 1837 (Coates, 1981), and there was channelization and bank enforcement of its major tributary, the Missouri River, by 1912 (Galat *et al.*, 1998). Areas of the

Upper Mississippi River floodplain were also affected by the construction of large dams and navigation locks, with habitat eliminated by permanent inundation (USA; Grubaugh and Anderson, 1988). Such projects expanded in number and scope with support from the US government, formalized by the Flood Control Act of 1936. This gave the United States Army Corps of Engineers (USACE) responsibility to build extensive levee systems along several large rivers to reduce flood risk and enable navigation for economic activity. Impoundments and diversions have been used subsequently to satisfy demands on water resources in the western US, providing for irrigation and human consumption. These alterations can now be found along nearly every major river of the arid US Southwest. A direct consequence of these management actions has been to greatly reduce the dynamic effect of seasonal floodplain inundation, either by design or unintentionally, and this has caused far-reaching detrimental effects in the unique riparian ecotone where terrestrial and aquatic zones meet (Naiman and Décamps, 1997).

Most of the above-mentioned modifications to channels and floodplains can be classified as channelization. This term refers to any of several methods, including: (1) straightening the channel; (2) resectioning the channel by widening and/or deepening; (3) levee construction; (4) bank protection, and; (5) clearing or snagging the channel by removing obstructions (Knighton, 1998). The intent of channelization is usually to provide flood control or enhance navigation, but it can also influence sediment transport, geomorphic features, vegetation, and ecosystem function. For example, channel straightening immediately causes a steeper streambed slope, and this increases shear stress, which often leads to channel degradation in the altered reach (Galay, 1983; Harvey and Watson, 1986). With this lower channel elevation, a lower water table in the adjacent floodplain often follows. This particular sequence of events has caused decline in

wetland and riparian vegetation communities and phreatophytes that utilize shallow groundwater (Bryan, 1928; Stromberg *et al.*, 1996). Such changes also weaken the hydrologic connection between channel and floodplain that is typical of natural alluvial streams.

Lateral connectivity is also lost through channelization projects due to the elimination of floodplain inundation. This loss is significant because when water leaves the main channel during high flow events, key processes of sediment transport and vegetative succession take place, and these shape the geomorphic features and ecosystem structure of natural riparian areas (Ward *et al.*, 2002). For example, management actions that reduced flooding along the Rhône River led to encroachment of vegetation that colonized side arm channels where flow was eliminated (Olivier *et al.*, 2009). Patterns of flooding have also been associated with plant biodiversity, such that riparian wetland sites in Alaska (USA) with the highest spatial variability in flooding frequency also had the highest plant species richness (Pollock *et al.*, 1998). Anthropogenic changes in the timing or spatial extent of floodplain inundation are also likely to affect vegetation communities of riparian areas because these species have adapted to natural patterns of change in water elevation (Lytle and Poff, 2004).

Additional studies demonstrate that channelization affects ecosystem processes like nutrient cycling and the fate of water-borne contaminants. In stream reaches that have been channelized, for example, there is less retention of coarse particulate organic matter (Lepori, 2005). Nutrient mobility is also less because the channel is poorly-connected to the floodplain (Junk, 1989; Bayley, 1995); export of dissolved organic carbon from the floodplain to the river channel occurs at a lower rate where floodplain area has been lost due to management activities in Australia

(Thoms, 2003). Processing of nitrogen in floodplains with and without setback levees was compared using models, and this showed that levees cause a decrease in total denitrification of 30-40% for floods with recurrence intervals of 2, 5, and 25 years; larger floods of 100-year and 500-year recurrence intervals had similar amounts of total denitrification with and without levees only because higher water elevations in these events breached the levees (Gergel *et al.*, 2005). In a separate study of nitrogen cycling, measurements in restored floodplains indicated that restoration increases denitrification of water delivered to the floodplains by seasonal high flow events (Sheibley *et al.*, 2006). The fate of contaminants is also expected to differ between floodplains that are inundated periodically and those that have been disconnected from the active channel in Western Europe (Lair *et al.*, 2009).

Recent studies have also highlighted the effects of channelization on fauna such as fish and aquatic macroinvertebrates. In highly-impacted rivers like the Rhône, Danube, Rhine and Meuse of Europe, fish guilds adapted to main channel habitat dominate in most reaches, whereas guilds that utilize the secondary channels found in wide floodplains are well represented only in the rare segments where the channel pattern and vegetation communities still indicate a high level of lateral connectivity (Aarts *et al.*, 2004). The influence on community structure of arthropods is demonstrated by studies in Japan. In channelized reaches of the Makkari River drainage of Hokkaido, abundance of riparian spiders that feed on emerging aquatic insects is less than in natural channels (Laeser *et al.*, 2005). A separate study in the same region found that channelized and unaltered reference reaches along the lowland Shibetsu River differed in hydraulic conditions and macroinvertebrate community structure (Nakano and Nakamura, 2008). These authors also noted that restoring a reach to its previous meandering configuration provided

additional shallow aquatic edge habitat, and utilization of these sites by macroinvertebrates gave rise to significantly greater species richness than in the channelized reach.

The organized elimination of habitat in floodplains by channel modification projects is now recognized to have negative consequences for not only ecosystems, but also human society. With this awareness, a new paradigm has formed in which the benefits that derive from properly-functioning riparian areas are recognized to have value, and are classified as ecosystem services. These services have been defined as “the conditions and processes through which natural ecosystems, and the species which make them up, sustain and fulfill human life” (Daily, 1997). The actual services that floodplains provide, for example, include cleansing water as it moves through the watershed and attenuating peaks in the hydrograph to reduce the extent of downstream flooding. The concept of ecosystem services helps quantify what the cost is of losing these natural functions, or what corresponding value would be regained by restoring them. This approach has been the basis for detailed conceptual models and quantitative estimates (Costanza *et al.*, 1997; de Groot *et al.*, 2002; Brown *et al.*, 2007). For example, the value to humans of the landscape’s capacity to regulate the distribution and quality of water that first falls as widely-dispersed precipitation has been estimated on an annual basis per unit area (Costanza *et al.*, 1997; de Groot *et al.*, 2002).

The extent to which valuable riparian zones have been degraded raises the question of what society should do, and the case has been made that conservation alone is not enough—restoration must also be part of the policy (Jähnig *et al.*, 2008; Opperman, *et al.*, 2009). Indeed, policies in place across Europe currently encourage restoration of floodplain habitat. Specifically, the

European Water Framework Directive instructs member countries to attain “good ecological status” for their rivers (Jähnig *et al.*, 2008; European Commission, 2000). One example of a river that has been recognized as being in dire need of rehabilitation is the Rhône in France. It had been managed primarily for navigation, energy production, and irrigation until the 1980s. Then efforts to restore hydrologic connectivity began, and abandoned sidearm channels were reconnected with managed floods and side channel excavation (Olivier *et al.*, 2009). In 1994 ecological endpoints were also incorporated into this plan, funded in part by the French government (Olivier *et al.*, 2009). In the USA, stream restoration to counter the effects of channelization and multiple other threats to healthy riparian areas was supported by spending an average of more than \$1 billion per year from 1990-2004 (Bernhardt *et al.*, 2005).

Methodologies for stream restoration are now beginning to be addressed in the scientific literature in several ways. Guidance can be found as general, prescriptive recommendations, and also as specific demonstrations of technique. One important goal should be to restore processes in degraded rivers rather than to choose fixed endpoints, such as a set physical form for a channel (Wohl *et al.*, 2005). This is because the driving forces in riparian zones, such as streamflow, are dynamic, and the physical form will continually adjust to these forces. Two processes studied for their historic role in the initial degradation and subsequent restoration of specific rivers are: (1) flow dynamics, and; (2) hydrologic connectivity (Kondolf *et al.*, 2006). These authors urge that flow regime changes be considered along with reestablishment of connectivity for restoration strategies. In a separate effort also intended to inform restoration design, a conceptual model of an ecologically-functioning floodplain is put forth, and this includes three key elements: “(1) hydrologic connectivity . . . (2) a variable hydrograph . . . and (3) sufficient

spatial scale . . .” (Opperman *et al.*, 2010). To account for these essential elements in restoration projects, the use of hydraulic models is advised, and the application of such tools by Williams (2009) is cited as an example (Opperman *et al.*, 2010). However, an alternative to hydraulic models for predicting inundation and floodplain connectivity is the use of satellite images and water balance equations; this approach has been demonstrated for large expanses of Australian wetlands (Overton, 2005; Powell *et al.*, 2008). This alternate method is attractive in part because it does not require the acquisition of detailed elevation data for the study area.

This need for high-resolution stream geometry information can now be met and applied to riparian restoration more easily because of recent advances in technology. When river restoration efforts began several decades ago, acquiring elevation data for hydraulic models required making physical measurements of the land surface. For example, a graduated grade rod placed on the ground in the floodplain was used with a transit to measure elevation at discrete points. Recent progress in remote sensing equipment and data processing, however, has made it possible to acquire high-resolution geospatial data using Light Detection and Ranging (LIDAR; Mertes, 2002). This technology has been used to guide efforts for rehabilitating salmon habitat in the Pacific Northwest (USA) by identifying river side channel sites with the highest likelihood for successful rehabilitation (Jones, 2006). A separate study used LIDAR to describe the channel and floodplain topography of existing salmon habitat, exploiting its capability to create continuous elevation models to characterize the fluvial geomorphologic features revealed at various spatial scales (McKean *et al.*, 2008). A recent review of LIDAR technology demonstrates that it is a versatile tool with innovative applications because it can characterize both aquatic and terrestrial habitats in ways never before possible (Vierling *et al.*, 2008).

Acquiring LIDAR data can be challenging, but recent advances in instruments, processing capabilities, and accessible archives continue to make this resource more available (Vierling *et al.*, 2011).

One area of study that links hydrology and ecology in a way that shows how impacted streams respond to and recover from anthropogenic change is the science of establishing appropriate instream flows. In rivers where dams or withdrawals have been implemented, concern for maintaining fisheries, endangered species, and entire ecosystems has encouraged substantial contributions of methods that link hydrology with biology (Petts, 2009). A specific tool that has developed from this research is the Physical Habitat Simulation Model (PHABSIM). It has applications similar to the study presented here because it is used to inform decision makers about aquatic habitat availability at different levels of streamflow and links habitat availability and biotic utilization (Bovee *et al.*, 1998). PHABSIM employs 1-D hydraulic models as a basis for habitat availability estimates, as does the current study. However, the present effort employs a continuous high-resolution surface model of stream geometry at the site rather than relying exclusively on cross sectional data, as in PHABSIM. This surface model increases the efficiency of adding stream geometry data to our hydraulic model, which also operates on elevation data in the form of cross sections. This increased efficiency may improve the accuracy of predicted water surface elevations because more elevation data can be included in the hydraulic model with little additional effort. More importantly, the surface model allows spatially-integrated visualization and analysis of hydraulic model results, because these can be exported directly to a Geographic Information System (GIS). This differs from the PHABSIM modeling approach, which achieves an areal representation of habitat availability by processing

results from representative cross sections within spreadsheets. Moreover, the current study uses elevation data from LIDAR, which is the most robust and explicit technique currently available (Lefsky *et al.*, 2002; McKean *et al.*, 2008; Vierling *et al.*, 2008).

Additional differences are that PHABSIM can be integrated into the comprehensive Instream Flow Incremental Methodology (IFIM; Bovee *et al.*, 1998), which has the functionality to optimize habitat availability for multiple species at once, and the typical PHABSIM application considers a stream reach longer than the one in the present study. Also, the IFIM method is concerned with loss or gain of habitat across a range of discharges to provide information for setting environmental flows on regulated streams, whereas the present study applies to an unregulated stream with a natural flow regime, and compares habitat availability for alternate channel geometries. Habitat is defined in PHABSIM for a specific organism, but in the current study the goal is to reestablish connectivity between the floodplain and main channel, and so inundation patterns and extent are of greatest interest. The goal of increasing lateral connectivity in the current design provides ample opportunity to reinstate fluvial geomorphic dynamics such as channel migration that have been identified by Richards and others (2002) as important for effective floodplain restoration. Reestablishing these processes should help develop ecosystem structure and function that support a mosaic of plant species adapted to such conditions, and which is similar to what would be expected if the site had not been affected by channelization (Gregory, 1991; Ward *et al.*, 2002; Hauer *et al.*, 2003).

This case study is a systematic approach to design and evaluate a stream restoration plan intended to increase aquatic habitat and lateral connectivity along a reach that has been

channelized. The site is located in semi-arid southwest New Mexico (USA) along the Upper Gila River, one of the last free-flowing rivers of the US Southwest. The site rehabilitation proposed and evaluated is the creation of a new overflow channel and backwater area in the presently disconnected floodplain. This reconfigured channel pattern is described by modifying a high-resolution elevation model of the existing configuration, which is built from LIDAR data and in-channel surveys. The assessment for potential habitat and lateral connectivity utilizes steady flow, 1-D hydraulic modeling of ecologically-important discharges to estimate the extent and pattern of inundation throughout the reach. The approach is unique for its use of software specifically designed to select ecologically-relevant flows (USACE, 2009a; Dunn and Hickey, 2003) and also because high-resolution surface models are developed to input elevation data to each hydraulic model. The surface models also allow spatially-explicit evaluation of the hydraulic model output, including the characterization of changes in spatial and temporal heterogeneity that could be realized with restoration. This comparison is intended to guide restoration efforts at the site, and also to describe a modeling technique that incorporates historic flow conditions to discern the effect that changes in channel geometry have on riparian and aquatic habitat.

## METHODS

### *Study site*

This project focuses on a 1.5 km reach of the Upper Gila River that drains 4,828 km<sup>2</sup> in semi-arid southwest New Mexico (USA; Figure 1). This river has perennial flow, and is one of the few in the southwestern United States that is unregulated. Annual mean flow at the site is 4.5 cms (158 cfs) based on 83 years of gage data from the U.S. Geological Survey (USGS)

streamflow gaging station 09430500, Gila River near Gila, located 25 meters upstream of the study site (USGS, 2010a.) Peak flows occur as a result of snowmelt in the spring, the North American monsoon in the summer, and dissipating tropical cyclones in the late fall (USGS, 2010b; Figure 2). There is also a period of predictable low flow in the early summer. The majority of watershed is in the Gila National Forest, including the Gila Wilderness Area.

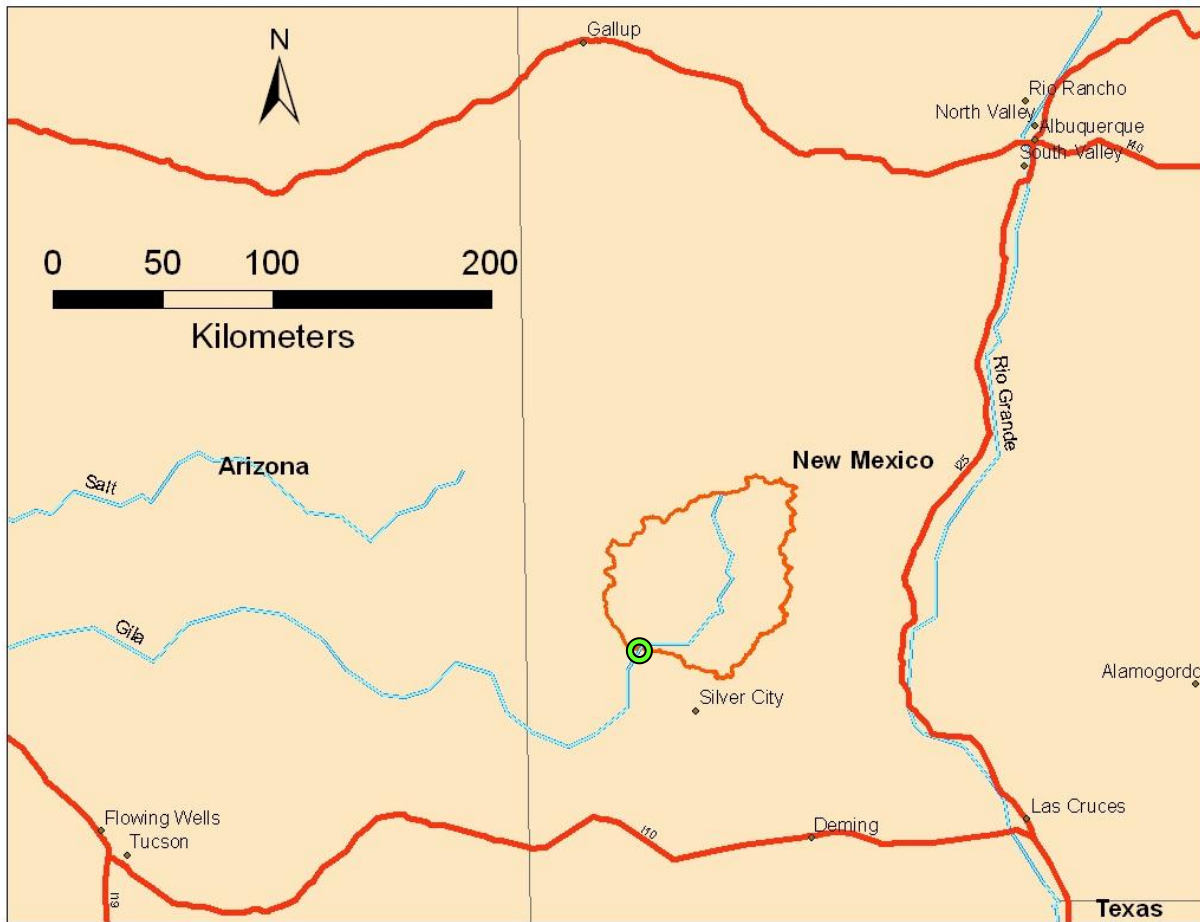


Figure 1. Study area location in the southwestern United States. Study site location is shown by a green circle, and the contributing watershed is outlined as an orange polygon.

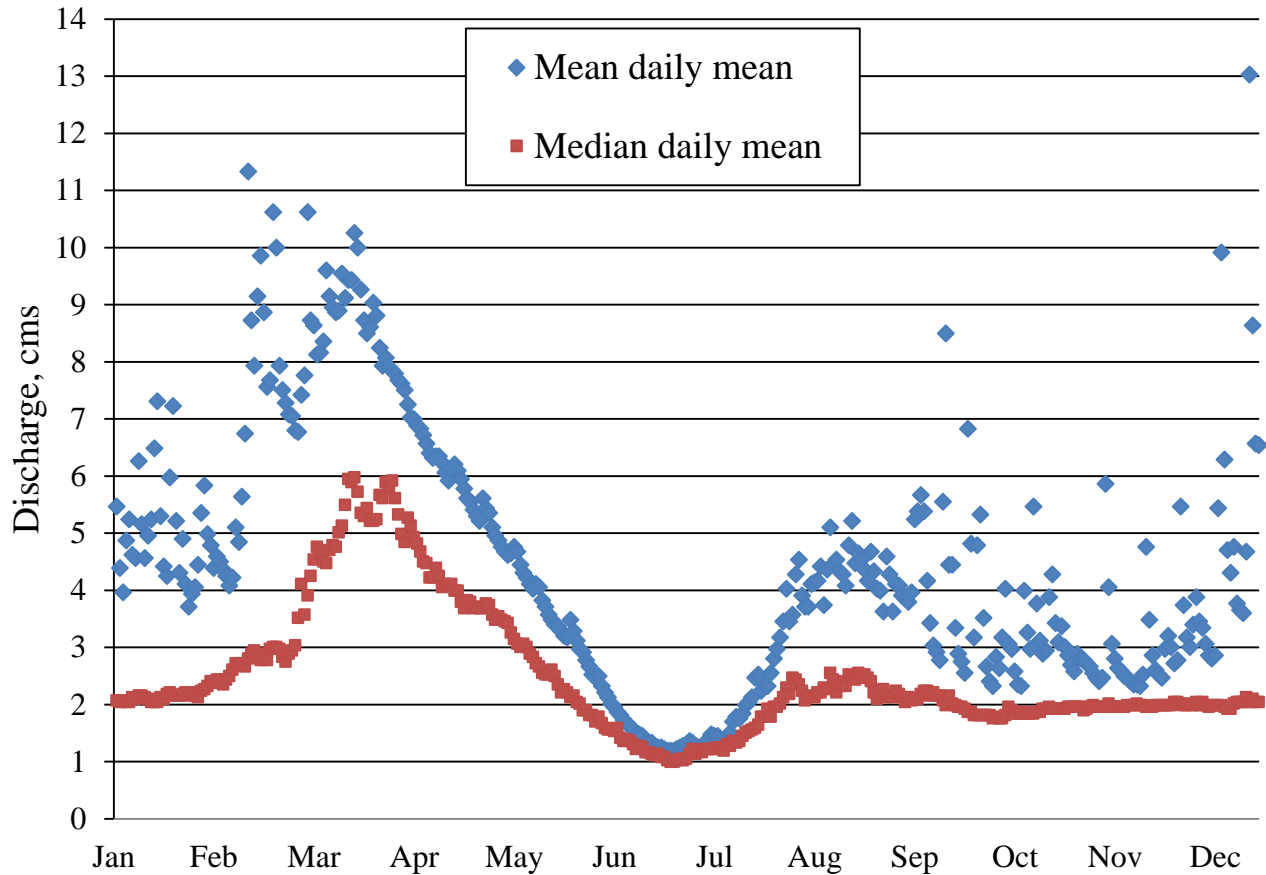


Figure 2. Daily mean discharge statistics for the period 1928-2010 (USGS, 2010b) at streamflow gaging station 09430500, Gila River near Gila, expressed as means and medians of mean daily flow.

The study reach was chosen to evaluate restoration potential because past activities have channelized the river, possibly in an effort to maximize the amount of arable land or to maintain operability of a streamflow gaging station. Farming ended at the site several decades ago, but this channelized form persists. An additional sign of impact currently observed at the site is incision of the streambed into the alluvium. This has been documented as a postchannelization response at other study areas (Harvey and Watson, 1986; Simon, 1989.) At this site, the stream banks at some locations are nearly vertical and measure 5 meters high. Also typical of channelized streams, this reach has almost no backwater areas or secondary channels, which offer diverse aquatic habitat elsewhere in the valley (Soles, 2003). These natural channel features have lower mean flow velocities and shallower depths that enhance ecosystem function

by providing sites for primary production of algae, growth of aquatic invertebrates, and refugia for young fishes. Among the species that could benefit from increased productivity in this riparian corridor are the endangered Southwestern Willow Flycatcher (*Empidonax traillii extimus*), threatened spinedace (*Meda fulgida*), and the candidate Yellow-billed cuckoo (*Coccyzus americanus*).

Although the river is currently unregulated, the study reach remains vulnerable to drastic changes in hydrology because of human demands for freshwater. Specifically, additional withdrawals up to 140,000 acre-feet per decade (172.62 cubic hectometers per decade) are an imminent possibility following the Arizona Water Settlements Act of 2004 passed by the US Congress (US, 2005; NMISC, 2006). A separate project still awaiting approval could potentially decrease discharge into the spring-fed headwaters of the Upper Gila River by removing 54,000 acre-feet of groundwater per year (66.58 cubic hectometers per year) from an adjacent endorheic basin (Blodgett, 1973; Myers *et al.*, 1994; New Mexico Environmental Law Center, 2011; Fleck, 2011).

#### *Site history*

To improve understanding of past human influence at the site, historical documents and photos are examined. One group of records evaluated is a series of primary documents from the period 1930-1960 titled Discharge Measurement Notes. These were produced by USGS personnel (USGS, 1930-1960) as handwritten notes on an official U.S. government form. This form is used primarily to record the flow velocity and cross-sectional area of flow to produce an accurate rating curve relating gage height to discharge. However, it also includes a section for

recording independent observations (“Remarks”). There were 1,016 Discharge Measurement Note forms completed from 1930-1960 for the gaging station immediately upstream of the study site, and each of these was reviewed. A second source of written information studied was the USGS Station Description for this streamflow gaging station. This is a single “living” document, which is maintained and constantly updated by the USGS (USGS, 2010c). One section of this document is titled “Establishment and History”, and is used to record streamflow-related events that occur at the site.

Additionally, two groups of historical photographic documents are used to understand changes in channel form. First, georeferenced aerial photos taken from 1935 to 2009 ( $n = 7$ ) were examined. Also, the USGS photo archive at the New Mexico Water Science Center (NMWSC) in Albuquerque, New Mexico contained several photos taken from the air and on the ground, from 1958 to 1972.

### *Geospatial data*

*High-resolution laser survey.* LIDAR technology was used to acquire elevation data for the ground surface. This was accomplished using a ground-based LIDAR scanner, the Optech ILRIS 3D with a pan-tilt base (Optech Inc., 2006). This line-of-sight instrument emits laser pulses and records their return, so that the relative location of surfaces in the landscape can be determined from the travel time, and the compositional characteristics of these surfaces can be evaluated based on the return strength of the pulse. This step was completed in winter, so that a minimum amount of foliage was present to obstruct the laser signal from reaching the ground. This technology is useful for describing habitat, because a single day of scanning can accurately

measure the location of millions of points in x, y, z space. For this project, the instrument was placed at three different vantage points to survey the study area.

To facilitate processing of the geospatial data, targets were positioned within the scene on steel posts so that spatial data collected by the scanner from the three vantage points, or scanning stations, could be related by common targets. The rectangular targets were made of white foam board with distinctive markings added using black vinyl tape. Targets ranged in size from 20 cm x 30 cm for those placed within 300 meters of the scanner, to 50 cm x 80 cm for those located at a distance of 800 meters from the scanner. These targets were laser-surveyed using the highest resolution possible, which was usually  $<2$  cm. The resulting data served a dual purpose during processing: 1) to allow data gathered from different locations to be merged by identifying common targets from more than one scanning station, and 2) to allow the digital terrain model (DTM) generated from the survey to be accurately georeferenced based on the targets' absolute coordinates, which were collected with global positioning system (GPS) equipment.

### *Processing LIDAR data*

*Parsing.* The first step in processing the LIDAR data was accomplished with the parser, which uses as input data the metafiles created by the Optech scanner during data acquisition. These consist of a binary file of the scan data, a file with the image of the survey scene, a description of scan settings, and operator notes. The primary output data from the parser are files suitable for use in PolyWorks, a program that allows manipulation, visual inspection and analysis of spatial data acquired by the scanner. Functions available during parsing include limiting the data by range or intensity, as well as data reduction to reduce file size (Optech Inc., 2006). For this

study, the parsing step allowed intensity of the data to be preserved by choosing the option “8-bit scaled”, then specifying the model of the pan-tilt base used in the field, and removing outliers.

*Merging and aligning.* This series of processing steps brings the parsed spatial data into the IMAlign module of InnovMetric’s PolyWorks software, measures the physical alignment between subsets of the entire dataset, and improves this alignment by moving the surveyed points according to constraints specified by the user (InnovMetric Software Inc., 2008a). The data is initially imported into the PolyWorks workspace such that each point is identified by its location in a Cartesian coordinate system and the intensity with which the infrared signal for that point returned to the scanner (i.e. “x, y, z, i”). The origin of the coordinate system is the LIDAR scanner.

Alignment of subsets of the data with each other is done at different scales (e.g. between datasets collected at a single scan station and also between data collected at different scan stations), and the workflow for this alignment process can be understood in terms of scanner operation during data acquisition. In the field, the instrument is first mounted on a tripod and rotating base, at which point the operator interactively specifies scan settings for the different parts of the scene, which can include up to 360° surrounding the scan station. Once the setup is completed and data acquisition begins, the instrument rotates on its base only when necessary to survey the next portion of the scene. This rotation introduces error into the data, but also allows a margin of overlap between areas surveyed from one rotational position to the next. These are the areas that are compared to accomplish the first step of alignment, which improves the integrity of the entire dataset collected at a single station.

The specific function that IMAlign software uses to do this is a best-fit alignment process. This permits the user to specify certain constraints, such as which points that will not be allowed to move or if some points should be ignored when calculating the best-fit. It may be appropriate to ignore some data points, for example, if they represent leafy vegetation that is constantly moving during the scan. After the best-fit alignment process has been performed for the specified number of iterations, the resulting fit between the subsets of data is described statistically by IMAlign. The two statistics used for this study were the measurement of mean error and the error histogram. The goal for mean error we chose was the nominal error of the scanner, which is approximately 1 mm. The error histogram describes the frequency of a given measurement error value for all points in the two independently-surveyed datasets that coincide in space. The mean and standard deviation are shown, and a uniform distribution is desirable. A skewed distribution often indicates that the alignment could be improved if the constraints of the alignment are changed.

An additional software feature that was used to visually assess the quality of the alignment between subsets of data was the error map. This map displays the measured error between overlapping points, which is presented as a color scale superimposed on the points in the scene. If a trend of increasing error can be seen along a border, or a larger error is seen in an isolated area, for example, then this is clearly not ideal and often indicates that the alignment can be improved. It should be noted that the points compared or aligned in any of these processes nearly always belong to a dataset with additional points, and so data for relatively large extents

of continuously-surveyed landscape can be aligned by inspection and manipulation of narrower areas.

The final step used to merge and align the laser-surveyed data in this study was to combine data collected at three scan stations into a common coordinate system. First, the compass bearing of the scanner as measured in the field at each of the three scan stations was used to orient each of the three merged and aligned datasets with respect to the cardinal directions. Next, an approximate alignment was made between these datasets using a function in IMAlign. This function served to bring one dataset into approximate alignment with another based on the user's selection of two points—one in each dataset—which represented the same point in space. These points were often chosen on the targets that were placed in the scene, and distinctive features in the landscape were also used. During this process, a single scan station from one of the datasets was chosen for the origin, and datasets scanned from other stations were brought into this common coordinate system. After each approximate alignment, a best-fit alignment between the datasets was performed as described above, and the error statistics were reviewed. After these two alignment steps were completed for data collected from all of the scan stations, the relative alignment of the entire group of LIDAR-surveyed points was fixed, and only rotation of the scene was allowed during the georeferencing operation described below.

*Georeferencing.* GPS coordinates were measured at 22 targets and 3 scan stations in the study site to aid in geo-referencing the DTM. These data were collected with a Trimble GPS Pathfinder Pro XH receiver, using the Wide Area Augmentation System (WAAS), giving accuracy of 30 cm or less (Trimble, 2009). The antenna was positioned atop a 2 meter range

pole over all features for an occupation time of approximately two minutes to collect a minimum of 30 satellite positions. The receiver measured horizontal position using a latitude/longitude coordinate system, and this was converted to Universal Transverse Mercator (UTM) coordinates with the online tool offered by the National Geodetic Survey (NGS, 2010). Elevation was measured as height above the ellipsoid, and was post-processed to obtain height above sea level with the GEOID 99 model, also offered online by the National Geodetic Survey (NGS, 2010).

Using these coordinates, an initial “huge translation” re-positioned the entire point cloud of LIDAR-surveyed points to near its georeferenced position, but did not apply any rotation. This was done in IMInspect, a second module of the InnovMetric PolyWorks software (InnovMetric Software Inc., 2008b). This brought the entire scene closer to final geo-referenced position by a spatial translation defined in UTM coordinates. The magnitude of this translation was equal to the GPS coordinates measured at the same scan station that had been conserved as the origin in x, y, z space throughout the merging and aligning processes. The reason this “huge translation” is done before fitting the data to the GPS coordinates measured at the targets is based on the capability of IMInspect to distinguish between small-number coordinate systems and large-number coordinate systems. The small-number coordinate system is how the scanner defines the data initially, and the maximum value depends on the range of the scanner, which was less than 1 km in this project. In contrast, the scale of distances that UTM coordinates define is typically thousands of kilometers. To accommodate these disparate scales with computing efficiency, the software uses both large- and small-number coordinate systems simultaneously on a single dataset, which allows the user to manipulate millions of geo-referenced points while maintaining accuracy and precision. The “huge translation” defines the large-number coordinate

system, and this allows the final geo-referencing step described below to be done with no loss of accuracy.

The final step in geo-referencing this dataset relied on the ability to identify several LIDAR-surveyed points with known GPS coordinates, and then move the entire scene in space to match these coordinates as closely as possible. This function in IMInspect is called “Align N Pairs of Center Points.” To utilize it, the LIDAR-surveyed targets were identified in the data by visual inspection, and a point was chosen near the center of each target. Once the target height above ground surface was corrected for, these center points were assumed to correspond to the GPS coordinates measured at each target. Therefore, a corresponding set of points was created from the GPS coordinates to serve as “destination” points, while those chosen from the LIDAR survey were the “source” points. By iteratively translating and rotating the entire scene, the software reduces the difference between several pairs of fixed destination points and movable source points to achieve a best fit between all point pairs specified. For this project, 10 pairs of points were identified for alignment.

*Bare-earth point classification.* Once the LIDAR-surveyed data were georeferenced, the remaining step in processing was to eliminate points that represented vegetation. This was necessary so that the surface generated from the data would depict only ground surface when added to the subsequent hydraulic model of streamflow. Initially, points representing vegetation were simply selected by visual inspection and re-classified as such interactively, within IMInspect. This was a practical solution for areas of the scene with a high density of LIDAR returns, because the form of the vegetation was easily perceived. It was a time consuming

process, however, and areas with a lower density of surveyed points due to obstruction of the LIDAR signal by vegetation in the foreground were difficult to classify because the overall form of the surface surveyed was poorly-defined. The intensity of the signal returned to the scanner helped to characterize these surfaces in some cases, as point intensity can be displayed in IMInspect, and vegetation generally reflects the laser back to the scanner with less intensity than does the ground surface.

As this manual point classification proceeded, its subjectivity and large time requirement led us to search for an alternate method. With the assistance of Gerald Bawden, USGS Research Geophysicist, the software program TerraScan (Terrasolid Ltd., 2010a) was ultimately used to perform this task. TerraScan employs a progressive approach to classifying points as ground surface, in which the lowest elevation points in the dataset are used first to define a triangulated irregular network (TIN) surface, and are classified a priori as ground returns. This model of the ground surface is gradually built upwards, with higher elevation points being added to it only if they meet user-defined values for distance above the TIN surface and angle to existing ground surface points (Terrasolid Ltd. 2010b). The algorithm used appears to be similar to that described by Axelsson (2000). To evaluate the TerraScan filtering process, the points classified as ground surface using TerraScan were imported into IMInspect for a visual comparison in the areas where manual filtering had been performed, and results were very similar. A final manual inspection of points used to define the ground surface and streambed for the hydraulic model was made after adding the bathymetry mesh, which is described in the following section.

### *Bathymetry*

*Channel survey and data processing.* Streambed elevations for the submerged portions of the channel could not be surveyed using LIDAR because the wavelength used by the Optech ILRIS 3D does not penetrate water. Therefore, to describe the channel geometry of the streambed for the elevation model, cross-sections were measured at 50 meter intervals for the length of the study reach (1,250 meters). At each cross-section, water depth was measured with a staff at 1 meter intervals along a transect perpendicular to streamflow. Relative streambed elevation was calculated by assuming that the water surface elevation was the same at all points along each cross-section. A total of 25 transects were described using this method. The streambed elevations were then imported into IMInspect as polylines, at which point the streambed transect elevations were positioned within the same coordinate system as the georeferenced LIDAR data. This was possible because the water surface elevation used to describe streambed elevations could be visualized in the LIDAR data. Detailed field notes and videos of landmarks at each transect were matched with objects visible in the processed LIDAR data to finalize transect positions in IMInspect.

*Bathymetry interpolation.* The streambed had to be modeled as a continuous surface for this project, but the 50 meter intervals between measured cross-sections were too large to render such a surface accurately if these data were used as the sole input. For example, the standard tools available in ArcMap (ESRI, 2010a) to produce a TIN from these points would simply connect them by straight lines, with no regard to the sinuous planform of the river between transects. In order to produce a more realistic model of the streambed, additional cross-sections and longitudinal profile lines were interpolated using a technique designed by Merwade and others

(2008a). This technique increases the spatial density of data while honoring the channel boundary between cross-sections. A custom tool that employs this technique has also been developed by Dr. Merwade for installation in ArcMap, and is available with a tutorial at his webpage (Merwade, 2008b). The input data required to use the bathymetry interpolation tool are 1) measured cross-sections as polylines, 2) a stream centerline as a polyline, and 3) the channel boundary as a polygon. These were all produced using IMInspect, exported as polylines, and then brought into ArcGIS.

### *Digital Terrain Model*

Once the georeferenced position of the bathymetry mesh and LIDAR-surveyed data were finalized, the choice remained of how to represent these in a DTM. The two options considered were a TIN or a GRID, because the software used to pre-process elevation data for the hydraulic model and post-process results required one of these two (USACE, 2009b). In choosing, consideration was given that the surface model influenced the analysis of habitat in two ways: 1) by initially defining the stream and floodplain geometry used by the hydraulic model to predict water surface elevations; and 2) by providing the frame of reference to interpret the hydraulic simulation results in terms of water depth and the areal extent of inundation. Therefore, the DTM had a central role, and this emphasized the need to preserve the resolution of the data as much as possible in the surface model. For these reasons, a TIN was clearly the best choice.

A TIN was made in ArcMap 9.3 (ESRI, 2010a) from the LIDAR-surveyed points, the measured cross-sections, and the interpolated mesh. The points were brought into the GIS environment as an ASCII file of x, y, z coordinates for each point, and a feature class of these

points was created. The measured cross-sections were introduced into the GIS as polylines defined in x, y, z coordinates, and the interpolated mesh was generated in ArcMap as described above. Once the TIN was made, it was reviewed for accuracy in ArcScene 9.3 (ESRI, 2010b), which displays data in three dimensions, and offers additional tools to navigate through the scene for detailed visual inspection. This revealed several spurious spikes and pits in the surface near the stream channel, which resulted from LIDAR-surveyed points that were incorrectly classified as ground surface returns. The spikes were likely from valid returns from overhanging vegetation, while the pits were artifacts generated by the laser signal being reflected or refracted by the water before it returned to the scanner. Their presence shows that inspecting the results of automated point classification routines is necessary to maximize data accuracy. The points responsible for these misrepresentations were deleted from the dataset interactively in IMInspect, and the remaining points were exported to form a new TIN. The functionality of IMInspect was superior to ArcGIS for this step, as it allowed the deletion of individual points, while also allowing the interpolated mesh to be imported and displayed as a visual aid. Finally, to increase the speed of displaying and manipulating the TIN in ArcMap, it was decimated to reduce the number of nodes using a specified Z tolerance of 10 cm.

*Stream geometry and alternate channel configurations.* The TIN surface is the source of essential stream geometry information for a hydraulic model of open channel flow. An initial elevation model that represents bare-earth of the current channel configuration is generated using the data and processing steps described above (i.e. LIDAR-surveyed bare-earth points and measured cross sections). To evaluate restoration potential at the site, a second surface model is created by adding overflow channels and backwater habitat to the original surface model. These

changes are made using the interactive TIN editing function of ArcMap 10 (ESRI, 2010a). The modifications are achieved by deleting TIN nodes in the disconnected floodplain, and then adding hard breaklines to define the streambed of new channels.

The choice of placement and form of the proposed overflow channels considers geomorphology, potential habitat gain, and current uses of the site. Specifically, the location is based on the evidence of past and present geomorphic forces that have shaped the site, including any channelization activity. The goal is to place overflow channels in a way that reproduces a structure and function similar to what would exist if channelization had never occurred. Present geomorphic forces are also a key consideration, as they should help maintain and enhance the physical form of the restoration. This importance of both past and present is reflected in the complementary analyses of historical documents and contemporary elevation data. The cross section form and longitudinal profile proposed for the overflow channels are designed to maximize aquatic habitat and increase habitat heterogeneity in the floodplain.

#### *Hydraulic model.*

*Software.* The purpose of modeling the hydraulics at the site is to estimate the areal extent and spatial pattern of inundation, as well as the total volume of water in the channel and floodplain. These values are calculated from the water surface elevations that the hydraulic model computes for the study reach using steady flow analysis for specified levels of streamflow. The model is built using the U.S. Army Corps of Engineers (USACE) Hydrologic Engineering Center's River Analysis System (HEC-RAS), which is a program that solves the energy and momentum equations for open channel flow to calculate water surface elevations at cross sections

throughout a reach (USACE, 2010). It uses a one dimensional approach to do this, and so lateral forces of streamflow are not considered. A companion software program used with this is HEC-GeoRAS, which is also designed and made available by the USACE (USACE, 2009b). It is installed as a plug-in for ArcMap 9.3 to extract stream geometry information from GIS data and build the hydraulic model in HEC-RAS. Following the steady flow analysis, GeoRAS also post-processes the HEC-RAS results so that they can be viewed and analyzed in the ArcGIS environment. The GIS data utilized in this study to generate the HEC-RAS models include a TIN surface for elevation and georeferencing, polygon shapefiles for landuse and ineffective flow areas, and polyline layers representing bank lines, levees, and flowpaths.

Two HEC-RAS stream geometry data files are used in this study. One file consists of a single reach, and the second has four reaches and two junctions. One of these junctions serves to separate streamflow from a single upstream reach into two reaches as it flows downstream, and this is referred to as a flow split. At this junction, the split flow optimization tool of HEC-RAS is used to calculate how discharge should be apportioned between the two downstream reaches based on iterative adjustments in discharge and comparison of the energy grade lines at the downstream cross sections. The stream geometry is described using 160 cross sections for the single reach, and 189 cross sections for the four reach plan.

*Boundary conditions.* A variety of assumptions about flow conditions can be made using HEC-RAS, and a mixed flow regime was chosen for this project, meaning that both subcritical and supercritical flow may occur during the simulation. Both types of flow can be observed at the study site. This assumption requires that boundary conditions be specified for the upstream and

downstream ends of the study reach, and that initial conditions also be given. Initial conditions will be computed by HEC-RAS using a steady flow backwater computation based on the entered flow data, and this will provide the initial stage at each cross-section. The upstream and downstream boundary conditions are normal depth. These are calculated within HEC-RAS based on the energy slope specified by the user at the upstream and downstream ends of the reach. To estimate the energy slope, the channel bottom and water surface slopes are estimated by querying the elevation model in a GIS environment. Using this method, the initial upstream boundary condition is based on a slope of 0.0004, and the downstream boundary condition uses a slope of 0.02 for all levels of discharge. Following the initial flow simulations, these values were modified to match the energy grade slopes calculated by HEC-RAS for each level of streamflow. This step allows more appropriate discharge-specific boundary conditions to be used in the hydraulic model (USACE, 2010).

*Choice and characterization of modeled flows.* The discharge levels modeled in this study are chosen from the full range of daily mean flows in the 83-year record available for this site. A total of 40 discrete levels of flow are included in the series of modeled flows, with a minimum of 1 cubic meter per second (cms), a maximum of 1,000 cms, and a median of 50 cms (Appendix 1). Lower levels of streamflow that have higher flow durations in the record are better represented than the less common higher flows. The record of daily mean flows is valuable for providing a clear picture of the magnitude and timing of streamflow at this site in the recent past (Figure 2). It is used to characterize the levels of stream discharge analyzed in this study with respect to seasonal timing and probability of occurrence, which are important to consider in restoration for the influence on ecosystem structure and function. To appreciate the multitude of

considerations in describing such flows, note that a review of indices designed to characterize streamflow records according to “biologically relevant” variables, addressed a total of 171 methods (Olden and Poff, 2003). From these methods, the researchers developed a list of categories to classify each index by its primary consideration: discharge magnitude, frequency, duration, timing, or rate of change during flow events. These are the same categories specified by Poff and others (1997) as comprising the “natural flow regime” that regulates ecosystem processes and ecological integrity of a river.

For the current study, we place the modeled stream discharges in a hydrological context with recently-developed software that allows each of the variables cited by Olden and Poff (2003) to be addressed explicitly. This software tool from the USACE Hydrologic Engineering Center is the Ecosystem Functions Model 2.0, or HEC-EFM (USACE, 2009a; Dunn and Hickey, 2003). This is essentially a statistical program that accepts time series data of daily mean discharge as input, and it can also be configured to analyze coincident changes in stage for a single location. The statistics that can be computed for discharge are duration, rate of change, percent exceedance, and time of year. The user specifies values to use in these statistical queries, and these values are intended to match the requirements of a single species or an entire group of organisms, such as benthic macroinvertebrates.

*Roughness coefficient.* HEC-RAS also requires that a roughness coefficient in the form of Manning’s  $n$  be assigned to all parts of the cross section. Estimating this empirical value accurately is a challenge that often requires professional judgment. In this study, information from several sources provide guidance, including reference photos, formulae for deriving  $n$ -

values with a composite approach, and previous studies of nearby sites. A report submitted to the NMISC by Mussetter Engineering Inc. (MEI, 2006) estimated Manning's n values, and measured particle size distributions for several areas upstream and downstream of the study site. This information helps form a robust estimate of Manning's n for the current study. Particle size data can be used to estimate roughness for in-channel locations, following the work of Limerinos (1970) in gravel and cobble-bed streams. For this approach, roughness height,  $k_s$ , can be estimated from the particle size that is larger than 84 percent of all bed material sampled,  $d_{84}$ , as:

$$k_s = 3.2 d_{84} \quad (1)$$

Roughness height can then be related to Manning's n over a wide range of depths using the Strickler Value,  $c_n$ :

$$c_n = n / k_s^{1/6} = 0.039 \quad \text{for SI units (Strickler, 1923; Sturm, 2001).} \quad (2)$$

An additional resource used to estimate roughness for this study is the compilation of photos by Barnes (1967) that shows the physical appearance of sites where Manning's n values were calculated based on measured flows and stream geometry.

#### *Habitat availability and floodplain connectivity assessment*

Aquatic habitat availability is evaluated as the areal extent of inundation and total volume of water in the reach for a range of stream discharge levels. Heterogeneity and floodplain connectivity are examined from a spatial and temporal perspective by qualitative and quantitative comparisons of inundation patterns. These analyses are done within ArcMap, and are based on hydraulic model simulation results exported from HEC-RAS and processed for use in a GIS environment by HEC-GeoRAS (USACE, 2009b; ESRI, 2010a).

## RESULTS

### *Site history*

Historical documents confirm that repeated efforts have been made to manipulate the planform and cross section of the river at this site. The most numerous references to channelization were found in the “Remarks” section of the Discharge Measurement Notes form. The “Establishment and History” section of the USGS Station Description for this streamflow gaging station also had valuable historical information, although it did not reflect most of the details that had been recorded in the Discharge Measurement Notes from 1930-1960. Table I summarizes the relevant excerpts from both sets of written documentation. Included are 6 instances of channel straightening, two of which specifically mention the use of heavy equipment. Entries are grouped to show that episodes of lateral channel migration usually preceded or followed channelization efforts.

Table I. References to channel modification events from handwritten notes on Discharge Measurement Notes (USGS, 1930-1960) and from the Station Description (USGS, 2010c.)

Date	Source document	Notation (summaries in parentheses)
1942-1948	Discharge Measurement Notes	(Seven dates note tractors, trucks, and wagons crossing at control, hauling ore, and causing shift on rating curve)
1/20/1949	Discharge Measurement Notes	channel has changed slightly...cut nearer...Right Bank & appears to have scoured some
3/09/1949	Discharge Measurement Notes	...found right A-frame washed out. A-frame & cable car are both down in water
7/16/1949	Discharge Measurement Notes	<b>Moving channel back to gage with bulldozer</b>
1/18/1952	Discharge Measurement Notes	channel has moved back to right where it was when bulldozer was used to cut new channel two years ago
8/15/1952	Discharge Measurement Notes	...old ditch heading ½ mile above is being reinstalled
7/14/1953	Discharge Measurement Notes	Center line for channel work by this station has been completed
9/03/1953	Discharge Measurement Notes	Channel straightening is getting started by this station
9/10/1953	Discharge Measurement Notes	Channeling work began today above station
11/20/1953	Discharge Measurement Notes	Channel work progressing by station work should be completed in a few days (note in margin: Shift? due to channel work)
11/27/1953	Discharge Measurement Notes	<b>channeling of river has been completed by station but channel control will shift for some time yet</b>
12/30/1953	Discharge Measurement Notes	Reconnaissance for another gage site was made today above present gage & one possible site about ½ mile above was located
4/17/1954	Discharge Measurement Notes	Total flow going by gage in old channel
1958	Station Description	<b>channel...is about 300' wide. Channel work done with a bulldozer, straightened channel leaving it about 90' wide with sloping banks nearly 12' high.</b>
6/23/1959	Discharge Measurement Notes	Moved up-stream to get above pump that was irrigating land on right bank
7/11/1960	Discharge Measurement Notes	<b>...Dozer work in channel along left bank at station</b>
12/17/1971	Station Description	<b>Channelization work has diverted flow back to original channel.</b>
11/15/1973	Station Description	<b>Channel work being done on control.</b>

**bold entries** indicate channelization events

Photographs of the site corroborate the written account of human impacts. Specifically, georeferenced aerial photos taken before and after the majority of events described in Table I demonstrate a straightened channel following these activities (Figures 3A and 3B.) Similarly, an aerial photo of the reach from 1966 in the USGS archive for the streamflow gaging station at this site has a caption that indicates the purpose of the photo was to document work that had been done on the channel (Figure 4.) Finally, the same archive contains a photo taken from the river bank opposite the gage in 1972, and it shows unambiguously that gravel had been graded with earth-moving equipment (Figure 5.) The Station Description narrative describes this activity in the excerpts that appear as the last two entries of Table I.

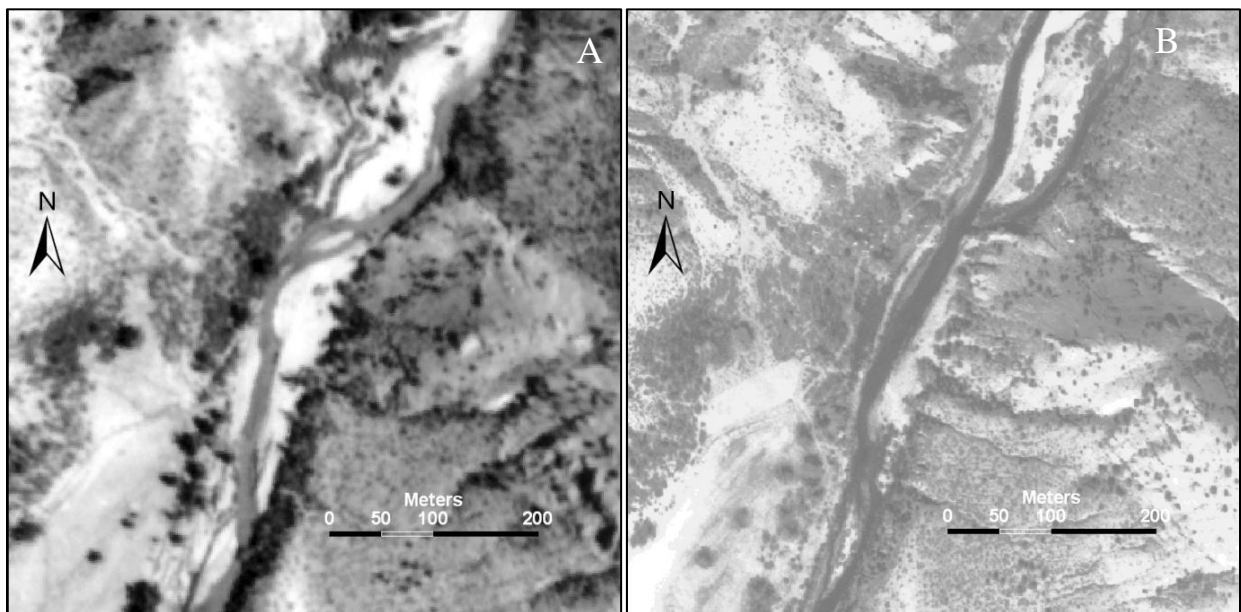


Figure 3. Aerial photos of the upstream end of the study site taken in (A) 1950, and; (B) 1965. Figure 3B shows the effect of several channelization events during the period 1953-1960, which are described in Table I. Direction of flow is north to south. Streamflow gaging station Gila River near Gila (09430500) is just above the center of the photos on the left bank (looking downstream.) Georeferenced aerial photo data provided by Ellen Soles.



Figure 4. Aerial photo of study site dated October 1966. The arrow appears to indicate location of stream gaging station, and the handwritten caption on the back of the photo reads, "Aerial photo . . . showing channel improvements." Direction of flow is from top to bottom. Visible to the right of the channel is a landing strip on a mesa, and an irrigation ditch in the floodplain. From USGS photo archive, New Mexico Water Science Center, Albuquerque, NM; photo by TE Yates. For distance, compare to same area in Figure 1.



Figure 5. 1972 photo at the upstream end of the study site, looking downstream from the right bank with the stream gage structure visible on the left. Note that unsorted gravel in the foreground has distinct ridges, and appears to be fill material recently-graded with heavy equipment. This is presumably the result of channelization work of 12/17/1971 referred to in Table I. Flow direction is from left to right. From USGS photo archive, New Mexico Water Science Center, Albuquerque, NM.

### *Geospatial data processing*

*High-resolution laser survey and data processing.* The total number of points surveyed during three days was slightly over 69 million, and only a small portion of these represented the ground-

surface. Woody riparian vegetation and grasses comprised a large share of the total points, and these were removed during data processing before the bare-earth elevation model was made.

*Merging and aligning.* The statistic used to evaluate the outcome of the best-fit alignment between scanned areas is the mean error. For the alignment of all scans made at a single scan station the goal was a mean error of 1 mm, which is the nominal error of the scanner. This was achieved in some cases, but mean errors generally ranged from 1 mm to 3 cm, with a maximum of 6.5 cm. The next alignment step was to combine these aligned data collected at three scan stations into a common coordinate system. The resulting mean errors for this ranged from 2-7 cm between one pair of datasets, and from <1-2 cm to align the third and final dataset.

*Georeferencing.* The original goal of using all 22 targets erected at the site to georeference the entire merged scene was not achieved because only 10 of these were defined well enough in the LIDAR survey to select a center point. After translating and rotating the entire merged scene to match the center points of these 10 targets as closely as possible to their GPS coordinates, the maximum error between the source and destination points was 0.67 meters, and for most point pairs this error was much lower.

*Elevation model and choice of alternate channel configurations.* The elevation model of the current site (Figure 6) serves an integral role as a source of detailed stream geometry data for the hydraulic model, and it is also helpful for selecting and visualizing areas where overflow channels and backwater habitat might be added for the restoration effort. A qualitative analysis of the elevation model in conjunction with site reconnaissance and study of historical documents

provides support for implementing these modifications in one or both of the two areas labeled in Figure 6.

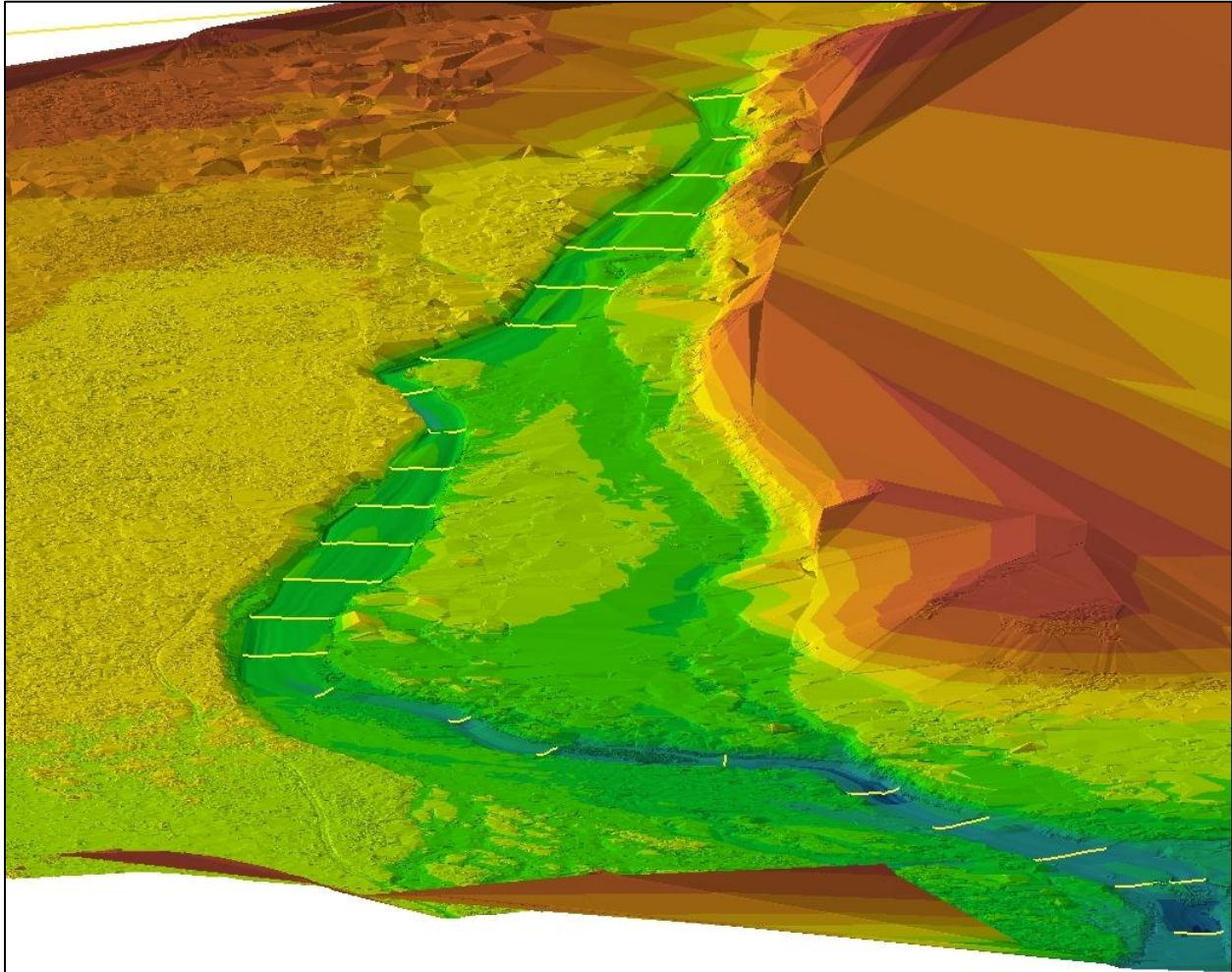


Figure 6. TIN surface representing bare-earth at site as it exists currently viewed in ArcScene (ESRI, 2010b). Yellow lines show the location of cross sections measured at 50 m intervals in the field to show streambed elevation. See the remnant overflow channel in area 1, which appears to have developed through fluvial processes. In area 2, a cut bank has developed, which is preventing lateral forces of streamflow from eroding the alluvium farther in the direction of the arrow (see text for additional explanation.) Direction of flow is from top to bottom; surface colors correspond to the elevation legend displayed in Figure 7.

The two locations to evaluate for new overflow channels were chosen after review of the documented history of the site and a geomorphic interpretation of its current form. Area 1 coincides with the upstream end of the study reach and is known to have been channelized over several months using heavy machinery, as described in the Station Analysis and Discharge

Measurement Notes documents (see Table I). A portion of a remnant overflow channel that seems to have been disconnected from the active channel by these channelization activities is apparent in the elevation model. This relic can also be appreciated visually during site visits, and appears in Figure 6 as a narrow band of green immediately below and to the left of the number “1.” The second area (“2”) is near the middle of the study reach, and currently has signs of focused, erosive streamflow energy. Specifically, a nearly-vertical “cut bank” measuring 5 m high has developed on the right bank (looking downstream) in area 2. Additional evidence that this feature is the result of ongoing lateral hydraulic forces is the presence of exposed tree roots along this bank, some of which belong to trees that have already fallen. These are the cues followed to investigate the restoration potential of initiating an overflow channel at this spot.

The locations of the two proposed channels are delineated in the plan view map of the site shown in Figures 7A-C. As indicated by Figure 7, I initially consider the effect of installing the two channels separately as well as in combination, for a total of three possible restoration scenarios. Each of these appear to have potential for rehabilitating ecosystem structure and function, but a final criterion is also used before evaluation with hydraulic models, which is to consider the merit of each plan with respect to compatibility with current uses of the site. The entire study reach passes through undeveloped land owned by The Nature Conservancy, and the dirt road that is visible on river right is not maintained, nor is it publicly-accessible. Therefore, it is not likely that widening the channel network in either area 1 or 2 would prevent any current uses of the disconnected floodplain. An additional concern is the USGS streamflow gaging station 09430500, Gila River near Gila, which is located only 25 meters upstream of the study site on the left bank. This gage would very likely become inoperable or unreliable if the passing

streamflow were divided among multiple channels. Such a loss of indispensable hydrologic data should be avoided, and so the two plans requiring excavation of an overflow channel near the gaging station in area 1 are too risky, and were eliminated from consideration. Therefore, the only restoration plan evaluated by hydraulic modeling is the creation of one overflow channel in area 2, as shown in Figure 7B.

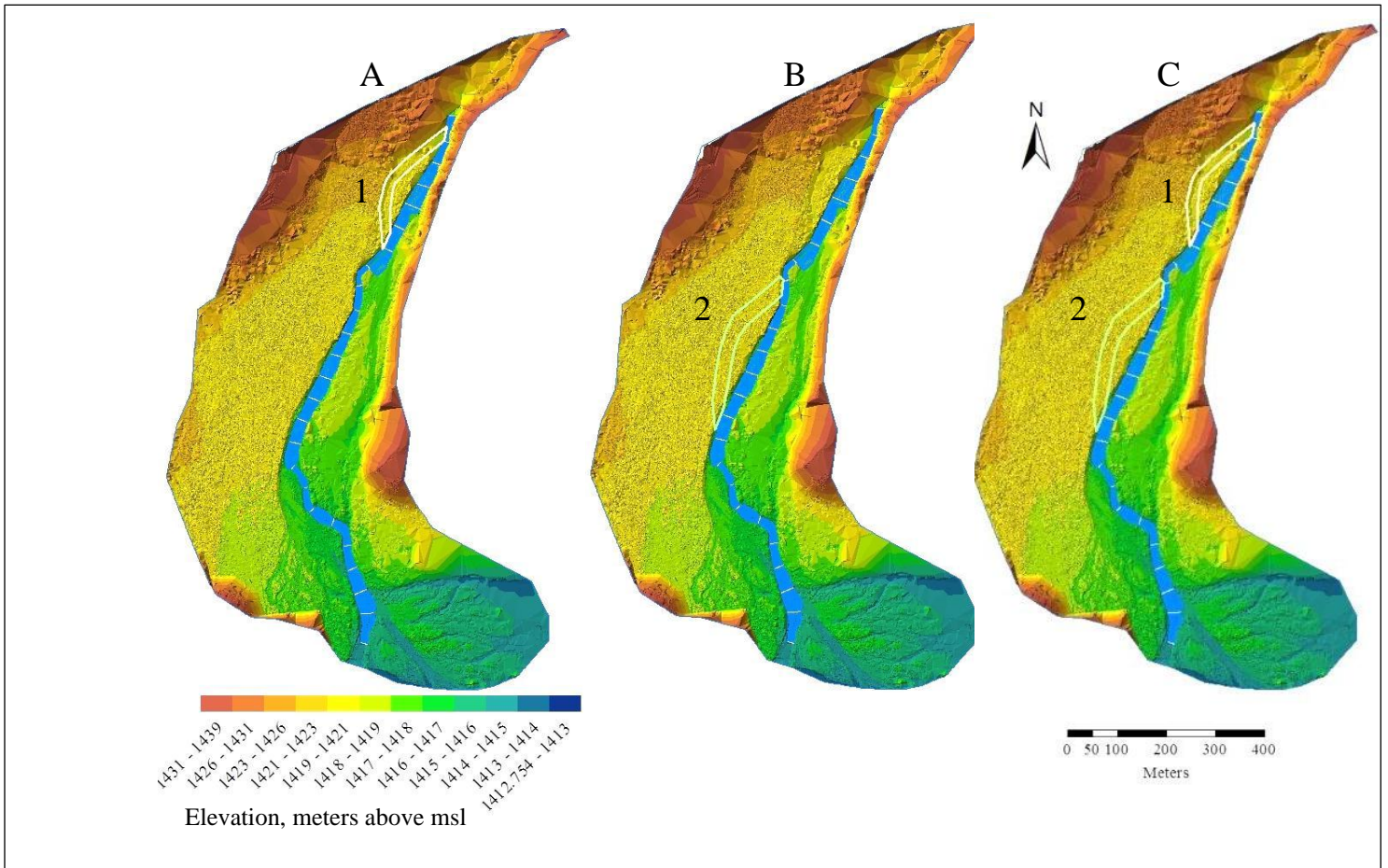


Figure 7. Plan view of surface model of the study site, with location of proposed overflow channels superimposed to indicate the three restoration scenarios considered. Note area 1 and area 2 correspond to the same areas in Figure 6.

The overflow channel is modeled as a trapezoid in cross-section with side slopes of approximately 11-12% (Figure 8). This slope is intended to be shallow enough to prevent bank failure and minimize degradation of the streambed. The longitudinal profile of the proposed

channel is determined by elevations in the existing main channel and in the large parafluvial zone on the opposite side of the river from area 2 (see Figure 6 and Figure 7). This parafluvial zone is partially inundated at moderately high streamflow, and the new channel in area 2 is designed so that it is accessed at this same level of discharge. When there is less streamflow, water will not flow the entire length of the new channel, but it should still provide protected backwater habitat where it reconnects to the main channel downstream. For this reason, the profile of the new channel will have a zero slope at the downstream end for a distance of 50 to 100 meters.

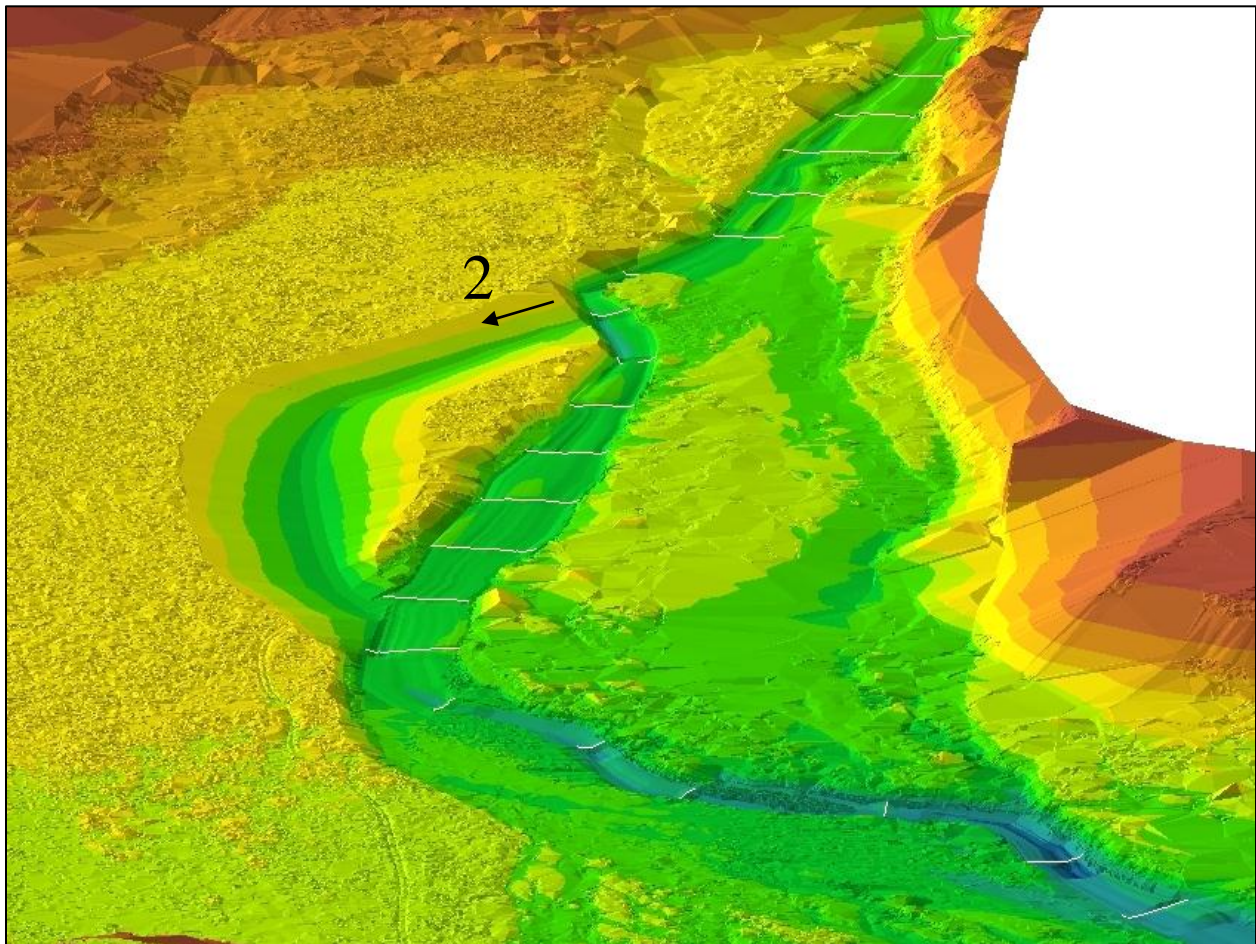


Figure 8. TIN surface showing location of overflow channel proposed and modeled for site (area 2) as viewed in ArcScene (ESRI, 2010b). Yellow lines show the location of cross sections measured at 50 m intervals in the field to show streambed elevation. Direction of flow is from top to bottom; surface colors correspond to the elevation legend in Figure 7.

### *Hydraulic model*

*Roughness coefficient.* Using particle size data from the Mussetter Engineering report (MEI, 2006) for “TNC Site”, which is approximately 8 km downstream from the study site, an estimated Manning’s  $n$  for the channel of  $n = 0.030$  was calculated using Equations (1) and (2). This differed from the value stated by MEI in its report, which specified  $n = 0.035$  for the channel. Their choice of this higher value seems appropriate after examining site photos, which show large woody debris present in the river. This debris would support adjusting Manning’s  $n$  upward based on “the relative effect of obstruction”, as presented in a composite calculation of Manning’s  $n$  (Chow 1959). In the current study, however, there is no large woody debris in the channel, and so a slightly lower Manning’s  $n$  is used in the channel. The roughness coefficients chosen for this study are summarized in Table II.

Table II. Roughness coefficients for hydraulic model.

Land cover type	Proposed Manning’s $n$
Bare ground with few shrubs (for in-channel and parafluvial zones)	0.033
Grasses and shrubs, 20-60% cover	0.036
Grasses and shrubs, 60-100% cover	0.040
Sycamores and cottonwoods	0.080
Dense willows	0.110
Sycamore/cottonwood/large woody debris	0.300

*Simulation of flooded area.* The total area of inundation simulated for the restored channel plan is higher than for the existing stream geometry at all levels of streamflow (Figures 9 and 10). As the modeled discharge increases, the difference in flooded area between the two site models also increases, with a maximum percent difference in flooded area of just more than 11 percent (Figure 10). This maximum percent difference occurs throughout a range of flows from 11-16

cms. The absolute difference in flooded area between the existing and proposed channel configurations increases by more than an order of magnitude, from 1,151 m<sup>2</sup> to 12,460 m<sup>2</sup>, through the discharge range of 1-400 cms (Figure 10).

At even higher discharge levels of 500-1,000 cms the hydraulic model becomes less representative of actual flooded area because the water surface extends so far into the floodplain that it reaches the ends of cross sections that define the stream geometry in HEC-RAS (Figure 11). When this happens, the behavior of the model is to create an artificial wall at the end of the cross section, and cause the water surface to rise higher than would be expected. This prevents the total area of inundation from increasing as much as it would otherwise, and the total flooded area is actually reported to be greater with the existing channel plan than with the overflow channel for the extreme upper range of modeled streamflow (700-1,000 cms).

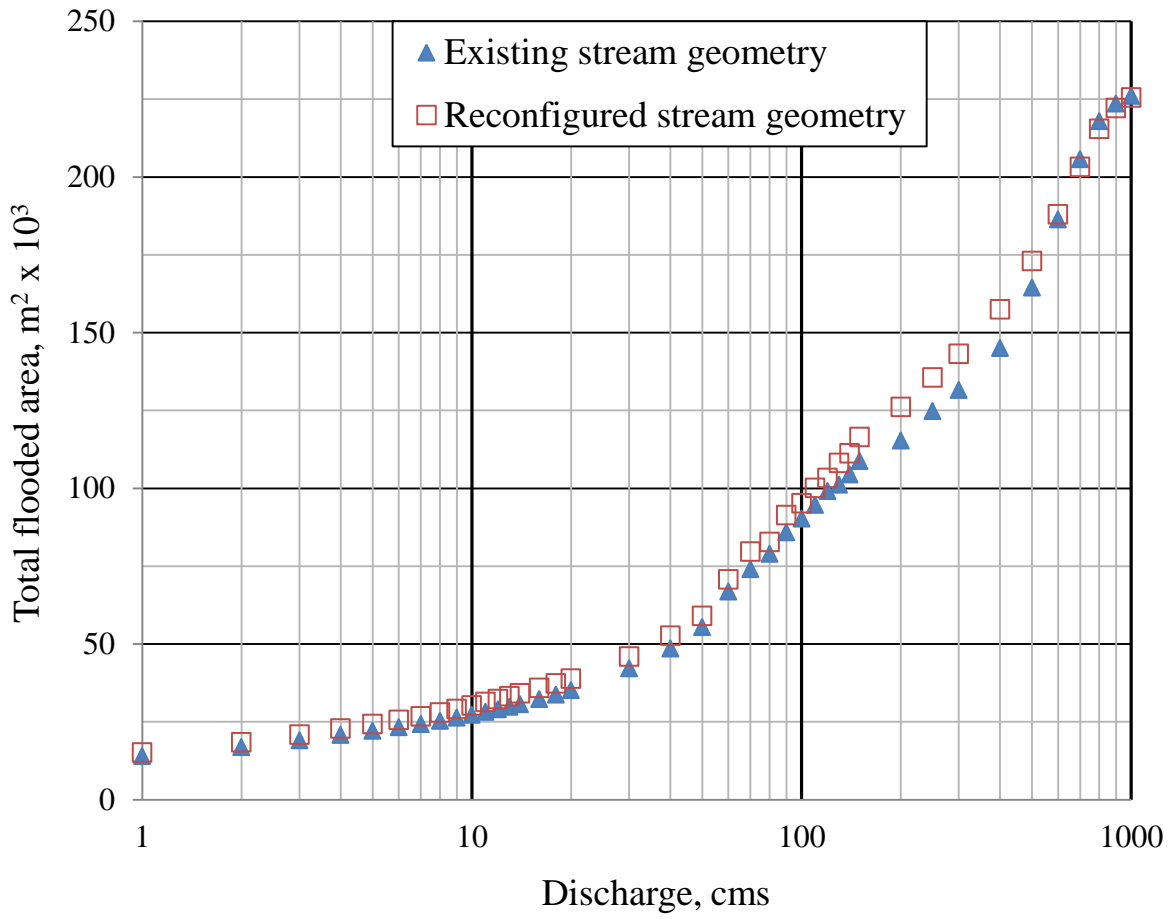


Figure 9. Total flooded area within study reach based on simulations in HEC-RAS and GIS analysis. The existing channelized stream geometry is contrasted with a modified geometry that connects the main channel to the floodplain.

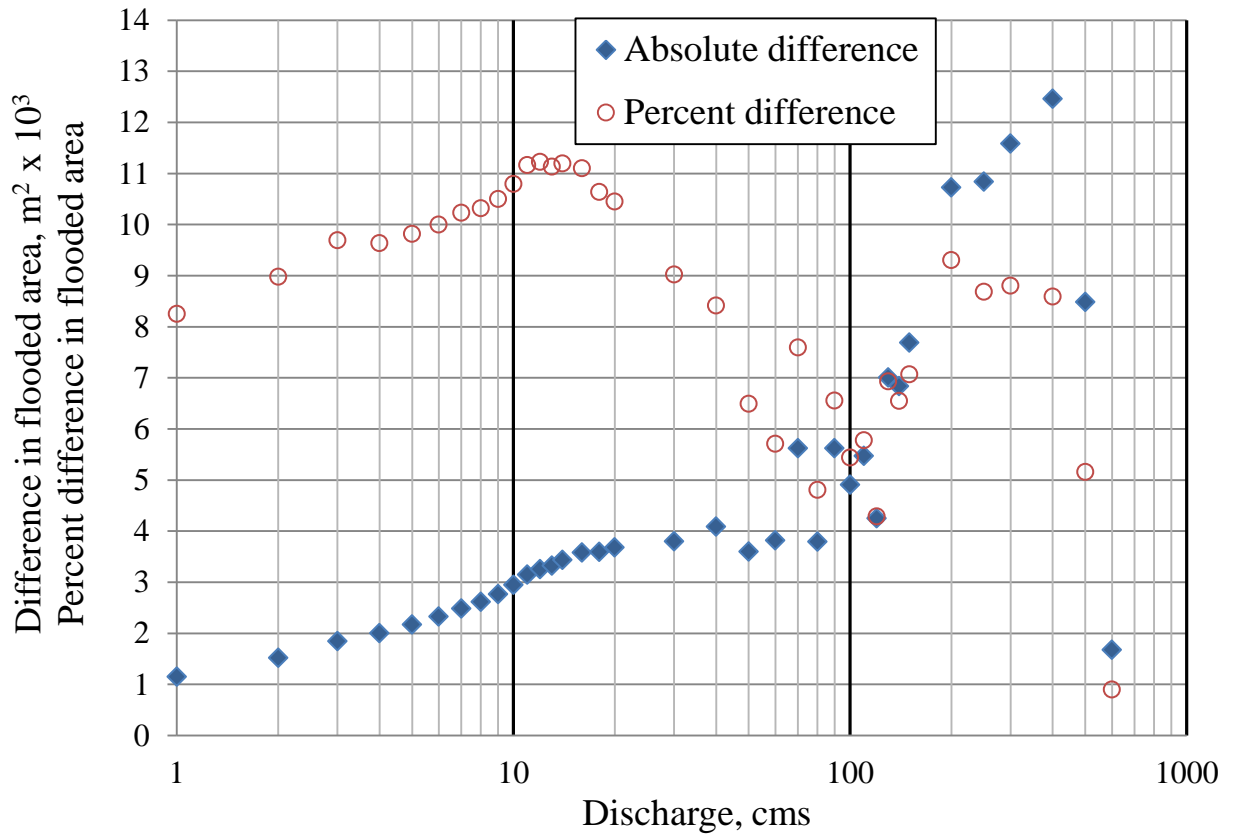


Figure 10. Absolute difference in flooded area and percent difference in flooded area between restored and existing channel and floodplain geometry based on simulations in HEC-RAS and GIS analysis.

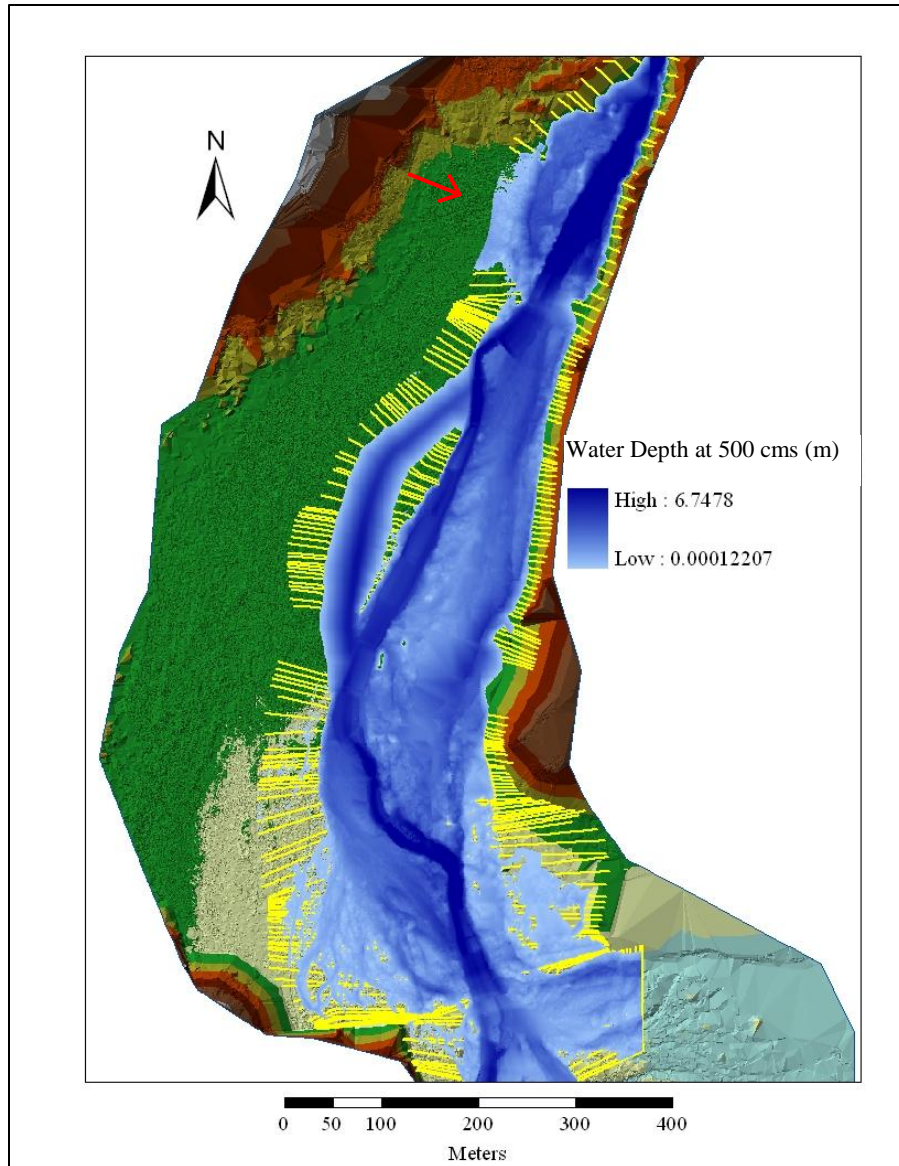


Figure 11. Mapped hydraulic model results for the flow of 500 cms with the restored channel plan. Note the yellow cross sections that define channel and floodplain geometry for the model. At the red arrow several of these are inundated to the end of the cross section. Flow is from top to bottom.

*Simulation of water volume.* The hydraulic models depict a similar trend for the volume of water present within the study reach as for the area of inundation, in which there is more water at each level of discharge when the overflow channel is included, and this differential increases throughout the discharge range (Figures 12 and 13). Unlike the values for area of inundation, however, this holds true even for very high flows in the case of total volume. This is what would

be expected since the hydraulic model does not allow water to leave the study reach when the simulated water surface extends to the lateral boundaries of the defined stream geometry. The percent difference in volume between the two channel configurations is also similar to the areal comparison because of the clear pattern shown, rising to a near maximum at a lower discharge of 9 cms before falling again as discharge increases (Figure 13). In the case of percent difference in volume, however, this zenith occurs at a lower discharge than for area, and the actual percent difference of 7.5% is slightly lower as well. These similarities between total volume and area of inundation are not surprising because they are both controlled by the same stream geometry and water surface elevation.

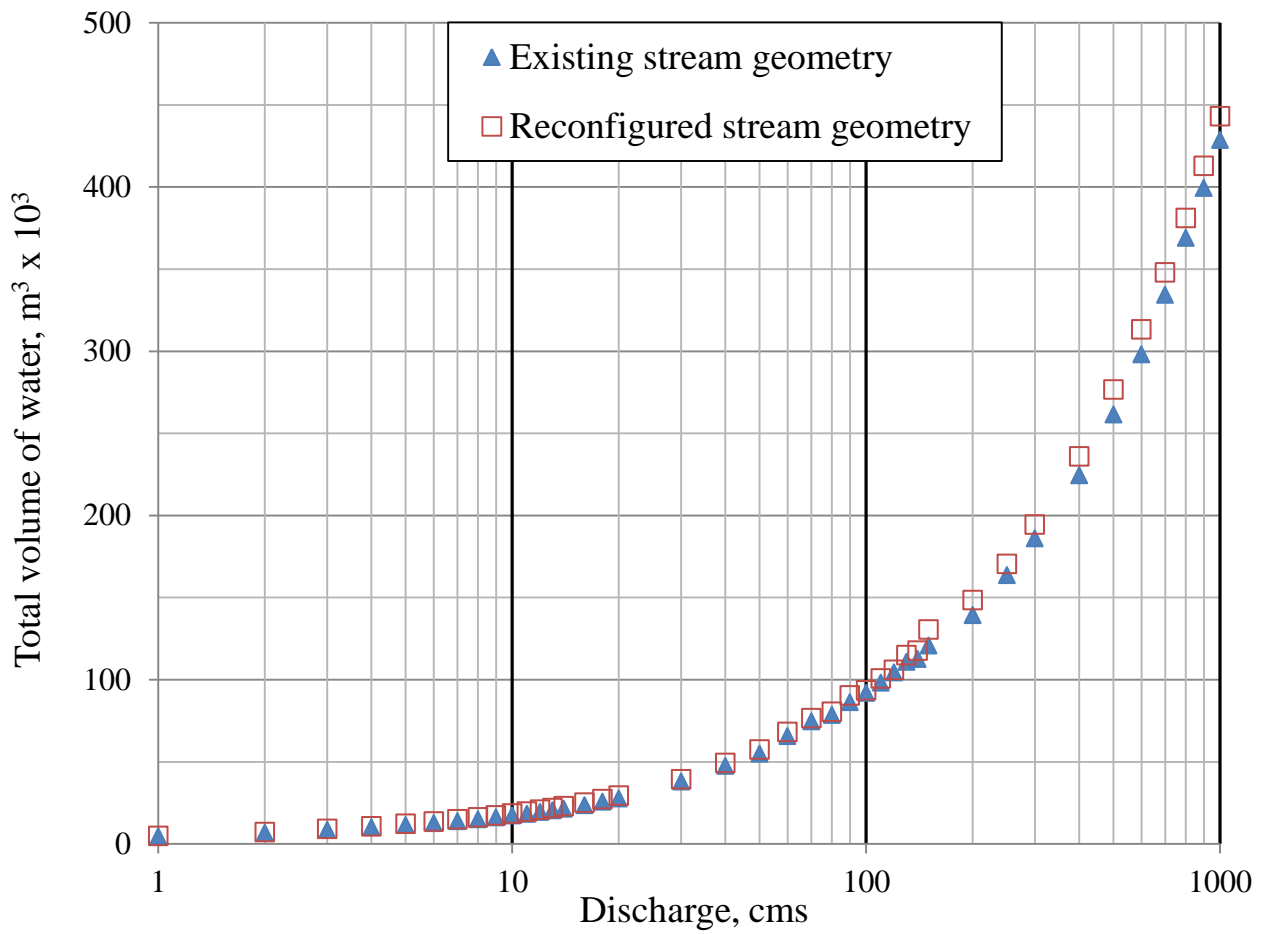


Figure 12. Total flooded volume within study reach based on simulations in HEC-RAS and GIS analysis. The existing channelized stream geometry is contrasted with a modified geometry that connects the main channel to the floodplain.

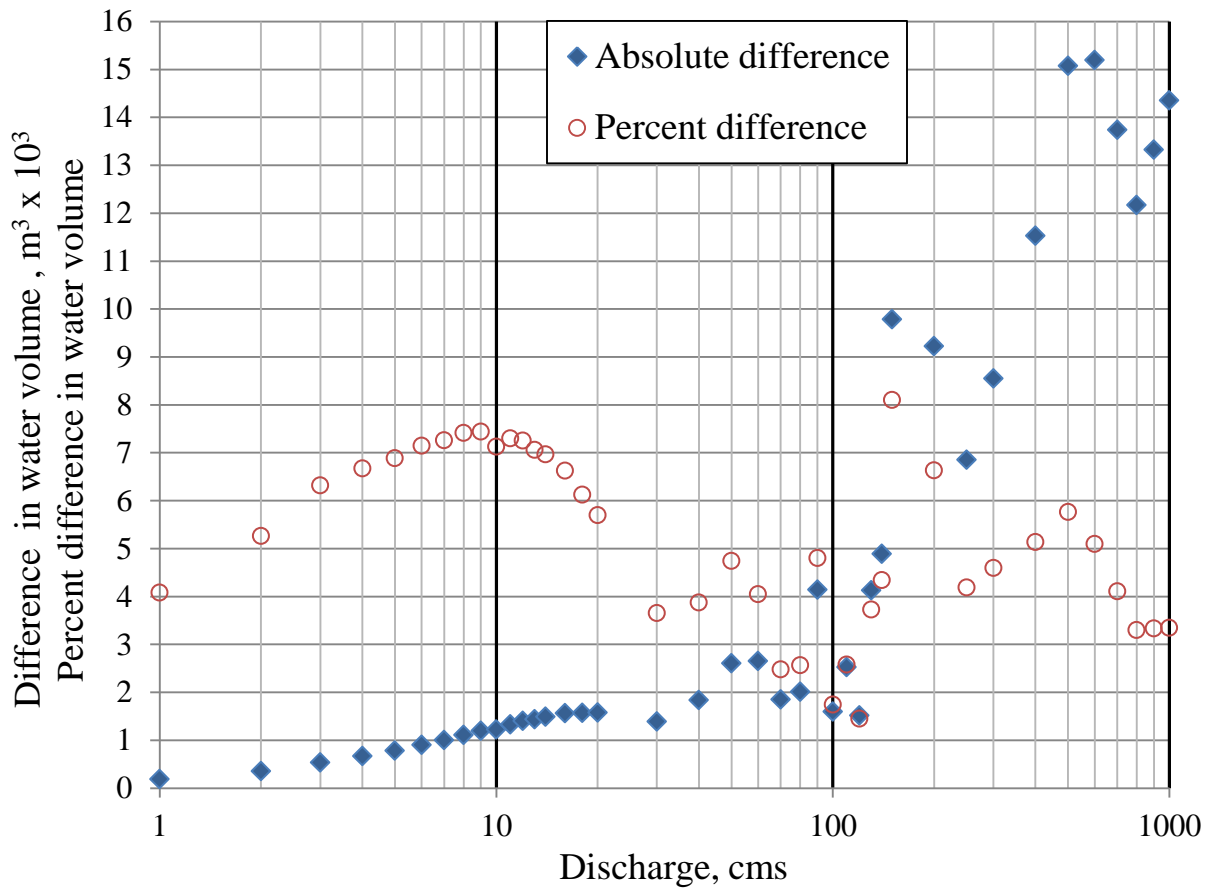


Figure 13. Absolute difference in flooded volume and percent difference in flooded volume between restored and existing channel and floodplain geometry based on simulations in HEC-RAS and GIS analysis.

*Simulation of inundation patterns and floodplain connectivity.* The differences in total inundated area and volume of water in the study reach between the channel reconfiguration plan and the existing site that are described above provide important information to evaluate the potential for restoration, but it would also be helpful to make more spatially-explicit comparisons between these two options. This can be done by considering how lateral connectivity between the floodplain and the main channel might be affected by restoration. To this end the flooding pattern in the overflow channel itself is examined, and the mapped results are also inspected for any effects this modification has on inundation in other areas of the floodplain. First, the flow

pattern within the new channel clearly provides new aquatic habitat in an area of the floodplain that is presently disconnected from the main channel. This happens in two ways, which can be appreciated in the mapped results of the hydraulic model. First, the downstream portion of the new channel is a site for protected backwater habitat at even the lowest modeled streamflow of 1 cms (Figure 14A). This backwater continues to increase in areal extent and depth to a discharge of 9 cms (Figure 14B). The maximum depth of the overflow channel as a backwater is 30 cm when 1 cms is flowing in the main channel, and depth increases to 85 cm for a discharge of 9 cms. At 10 cms the upstream end of the overflow channel is accessed by water from the main channel, and provides habitat and additional connectivity in the floodplain as a flowing channel at higher discharges.

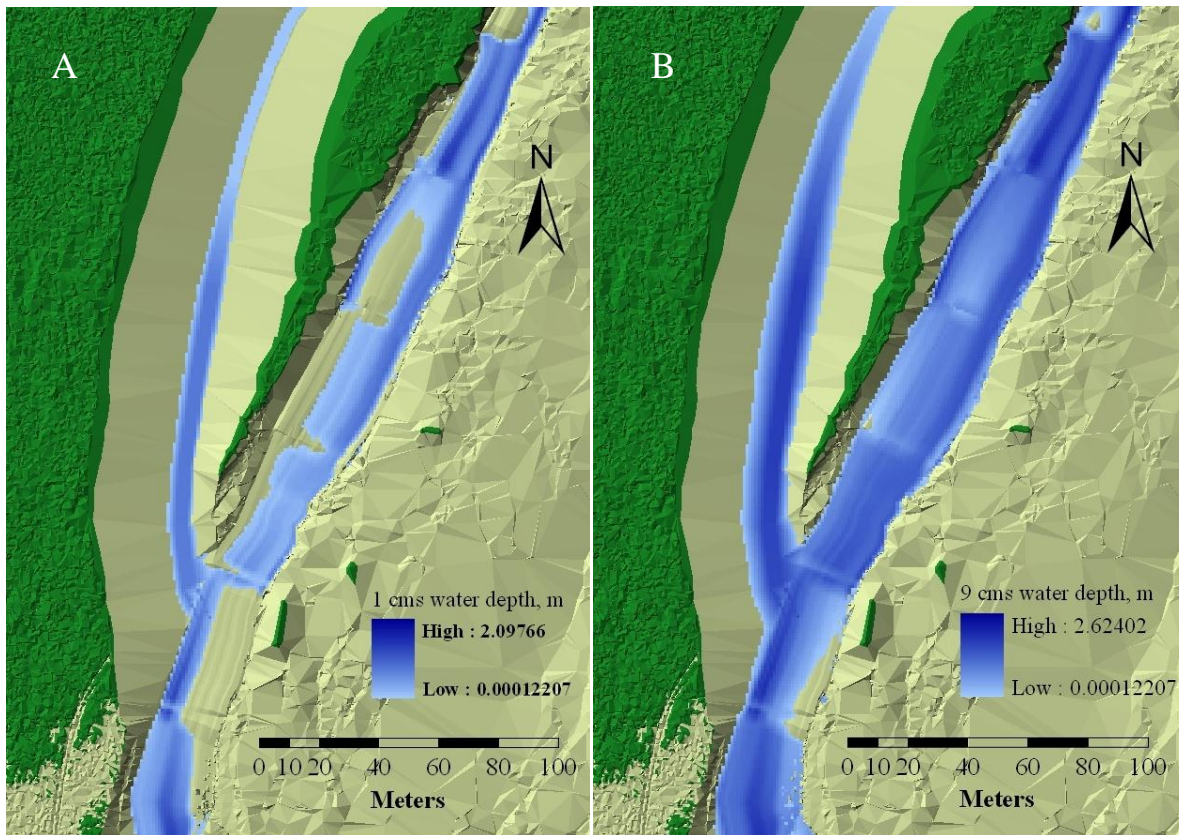


Figure 14. Water surface formed by a backwater in proposed overflow channel, which extends to the left of the main channel. Shown are the water surfaces simulated for 1 cms of flow in Figure 14A, and for 9 cms in Figure 14B. Flow in main channel is from top to bottom.

The indirect effect of a new overflow channel that can be explored by visually inspecting the mapped results of the hydraulic model is how the new overflow channel alters flooding in areas where overbank flow currently occurs. For example, on the opposite side of the main channel is a large parafluvial zone that shows evidence of periodic inundation. If present inundation patterns are affected by a new channel, then output from the model should indicate this. There is in fact a discernible difference at certain levels of discharge. Figure 15 shows the simulated water surface (blue) overlaid by the same surface for the restored configuration (black), while the only elevation model visible is for the restored configuration. As flow climbs to 10 cms, the existing parafluvial zone already has an isolated pool approximately 150 meters long and 10 meters wide (Figure 15A), while water has just begun to enter the overflow channel. At a higher level of discharge, flow of 30 cms inundates the isolated pool and reconnects it to the main channel in both configurations (Figure 15B). A slight difference in flooded area between the two configurations at 30 cms can be appreciated in the parafluvial zone as an irregular margin of 2-6 m around the edge of the water. This represents area that floods in the existing configuration but not in the restored configuration. Figure 15C depicts a much higher discharge of 80 cms, which inundates a much larger portion of the parafluvial zone for both configurations. The margin of blue that shows area not flooded due to the presence of the overflow channel has also increased in extent although not considerably so. Two conspicuous areas of blue are also interpreted as a lack of flooding because of restoration, but their odd straight edges are an artifact of the way HEC-RAS defines stream geometry in cross sections rather than an accurate representation of precisely where the floodplain will not be inundated. At a discharge level of 100 cms (Figure 15D) the difference in flooded area due to implementation of the restoration plan is essentially unchanged from Figure 15C, but there is considerably more area inundated at this higher

discharge. In addition, the flood water is now connected to the main channel at the downstream end of the parafluvial zone.

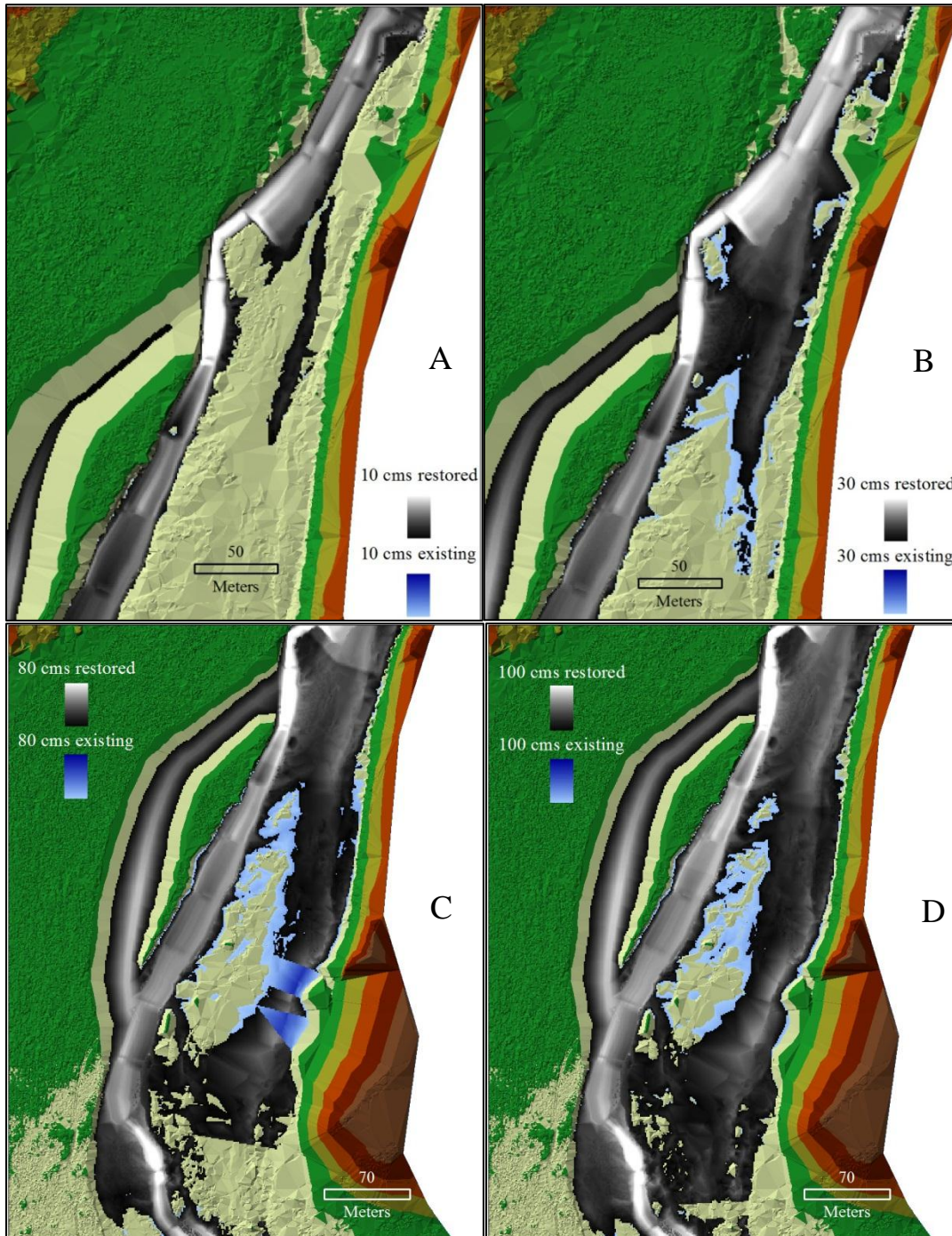


Figure 15. Simulated water depths illustrating flooded area and differences in inundation patterns. The black to white surface represents the simulated water depth for the restored configuration and the underlying blue surface (mostly obscured by water depth layer for the restored configuration) depicts water depth for the existing configuration. The visible blue surface represents area that is not flooded with the restored configuration but is flooded for the existing configuration.

A final GIS query of the model results is made to determine how the restoration would enhance floodplain connectivity. This is to measure the maximum width of the flooded area for the existing and reconfigured plans. Results indicating the position on the reach of each measurement are shown as labels in Figure 16. At a discharge of 10 cms the maximum flooded area of the restored configuration is 52 m wider (Figures 16A and 16B), and for a discharge of 100 cms the maximum width is 57 m wider with restoration. These distances are comparable because they primarily represent the same lateral distance across the floodplain to the overflow channel. For the lower flow of 10 cms this distance is an increase of 163%, and for the 100 cms it is a 40% increase.

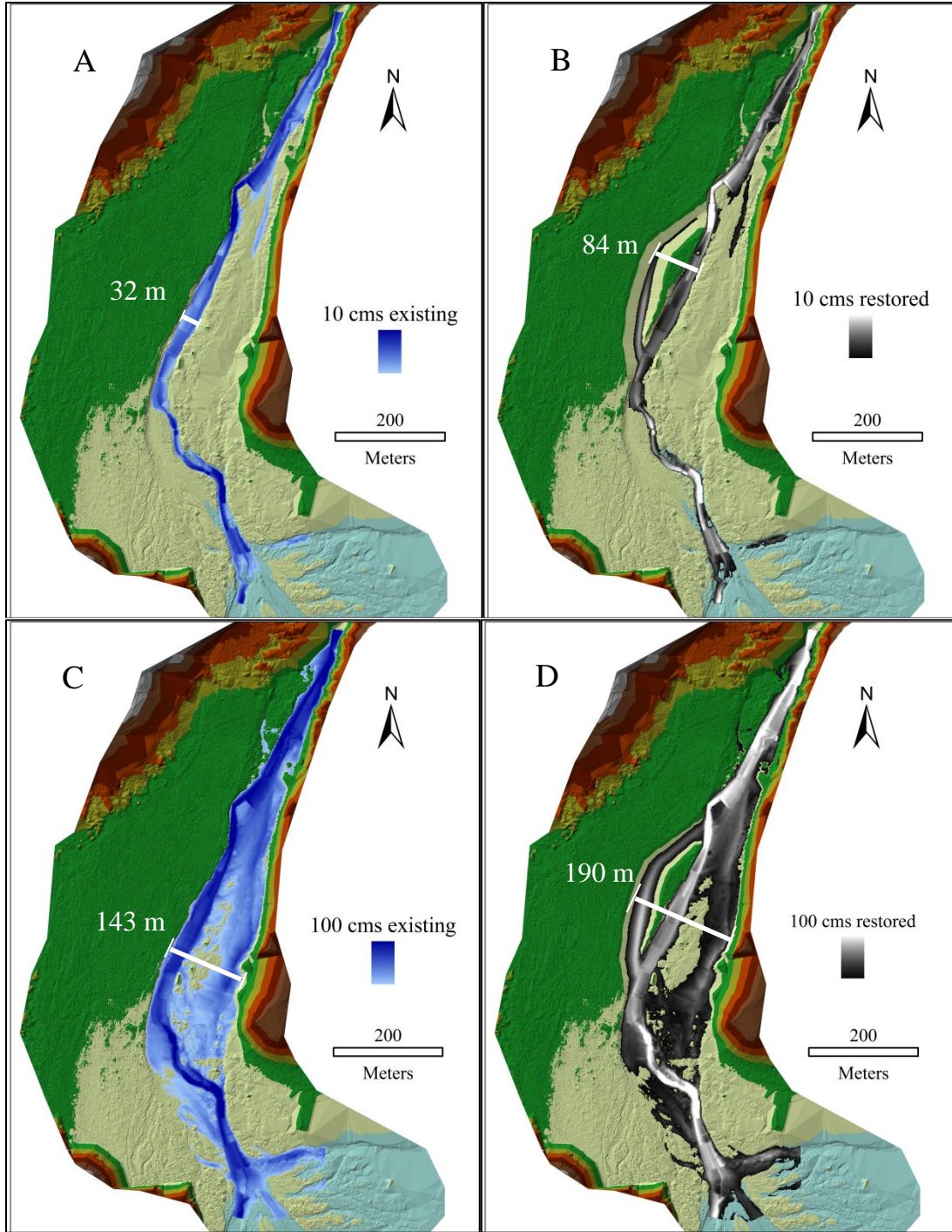


Figure 16. Plan view of study site showing maximum width of flooded area (in white) as measured across the water depth layer for the existing configuration (16A and 16C) and the restored configuration (16B and 16D) at 10 cms of discharge and 100 cms of discharge.

*Characterization of flows.* The role in the natural flow regime of the stream discharge levels used in the hydraulic model is clearer when the 83-year record of daily mean flows is described by seasonal statistics. Results of querying the record by this method using HEC-EFM may give a better understanding of which discharge levels are most relevant during each seasonal flow period. The individual periods analyzed are spring snowmelt (March 1-April 30), summer low flow (May 1-June 30), summer monsoon (July 1-September 30), and the winter season when the remnants of tropical cyclones can bring substantial precipitation to the region (November 1-February 28). Figure 17 shows the results of these analyses, identifying the magnitudes of daily mean flow that are expected to occur at the specified exceedance levels for each period.

The three periods that typically have higher than normal flows are grouped together on the chart (i.e. snowmelt runoff, summer monsoon, and tropical cyclone arrival) with values being most comparable at exceedance levels of 50, 25, and 10 percent. However, there is a prominent switch from below 50% exceedance to above 50% exceedance, in which the summer monsoon period has the highest flows for high exceedance levels, and the period of tropical cyclone arrival has the highest flows for low exceedance levels. For the summer low flow period, the computed streamflow magnitudes are below 10 cms for all but 5% and 10% exceedance, whereas the other three periods have 24-42 cms at the 25% exceedance level. The curve based on the entire year has considerably larger flows for all exceedance levels, indicating that numerous large flows also occur outside the seasons chosen for analysis.

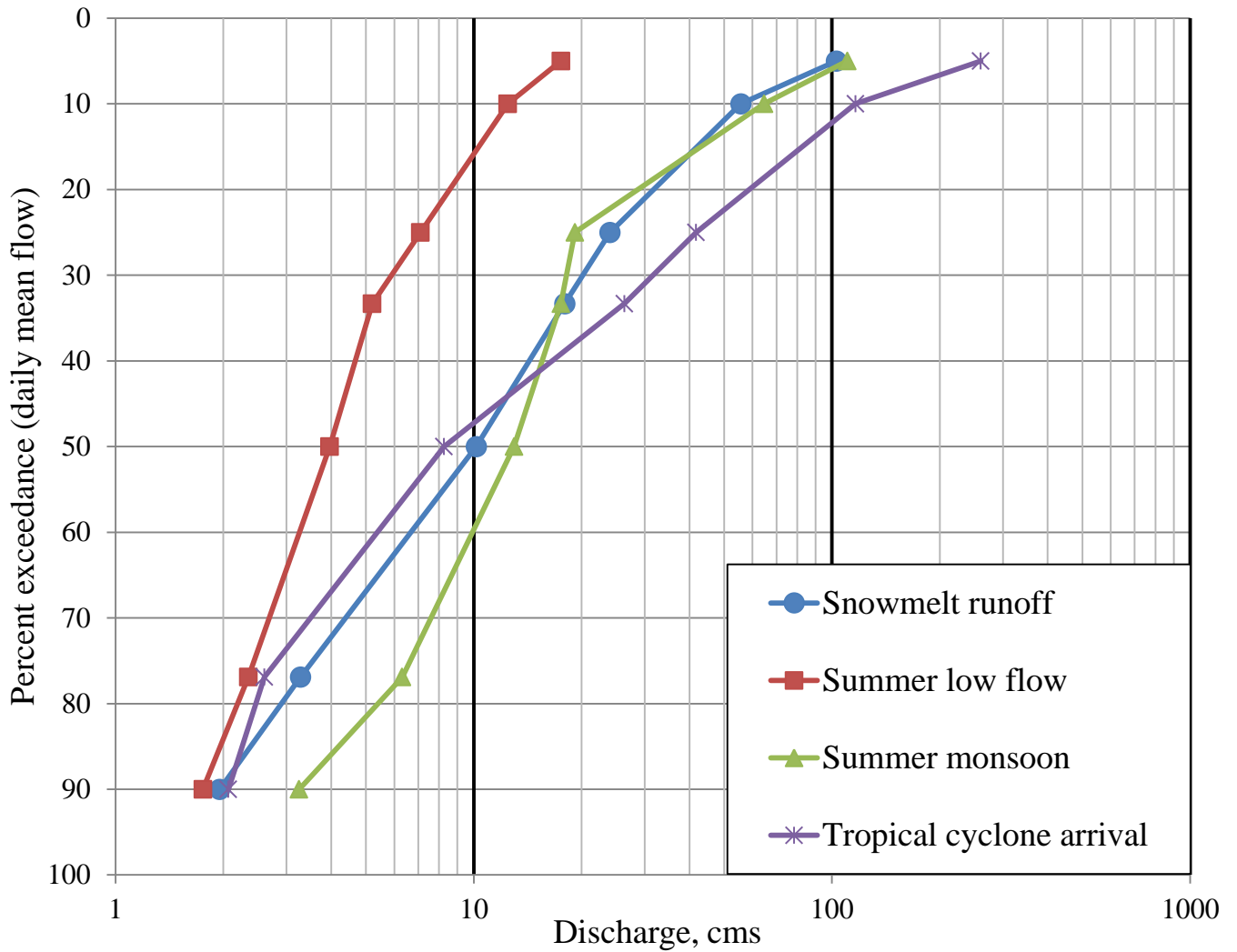


Figure 17. Percent exceedance analysis of daily mean flows by season for the period 1928-2010 (USGS, 2010b) at streamflow gaging station 09430500, Gila River near Gila, as calculated by HEC-EFM (USACE, 2009a).

## DISCUSSION

The results in Table I clearly show that the reach has been channelized repeatedly. The motivation for this work is not described in detail within the documents, but a few of the comments indicate a concern that the main channel is migrating away from the streamflow gage located immediately upstream of the site. If the channel were maintained next to the gaging

station in a static position, then it would allow the gage to accurately measure streamflow. A second possible motivation for channelization of this reach could have been to maximize the amount of water available for downstream users. This is certainly a likely explanation for the actions described in Table I from the late 1940s and 1950s through 1956, because drought conditions prompted channelization during this period along another river in New Mexico, the Rio Grande, in order to move water toward specific agricultural uses and to meet compact delivery requirements. Finally, a previous landowner may have undertaken or supported channelization efforts in an effort to maximize the amount of arable land and increase agricultural production in the surrounding floodplain.

The performance of the hydraulic model and the accuracy of the elevation model are both good. For example, the higher discharge levels of 500-1,000 cms that are too high to be represented accurately due to the inundation of the ends of cross sections are also extremely high in comparison to what has been observed during the 83-year streamflow record. Specifically, 500 cms is a peak annual flow with a 2.6% exceedance, making it a 38.5 year flood, and 1,000 cms is bigger than the largest peak flow ever observed at the site, which was the catastrophic flood of 996 cms that occurred on December 28, 1984. In terms of daily mean flows, the 500 cms level was only exceeded on two days in the period of record. Output from the hydraulic model also confirms that geospatial data gathered in the LIDAR survey is interpreted accurately. This is substantiated because the slope of the water surface calculated by querying the LIDAR point cloud matches the energy grade slope calculated by HEC-RAS for the discharge that was present on the same day the LIDAR survey was completed.

The primary goal of designing and demonstrating the performance of a restoration plan that provides increased aquatic habitat and floodplain connectivity is met by this project. The proposed modification of creating an overflow channel has been shown to add flooded area, additional water volume, and a wider floodplain to the site at all discharge levels modeled. Flooding simulations show specifically that the backwater area of this new channel increases available habitat in the study reach by more than 10% at flows below 10 cms, which is also the level of discharge that first accesses the upstream end of the channel (Figure 10 and Figure 14). Creating more habitat when discharge is less than 10 cms is a key feature of this plan for several reasons. From a hydrologic perspective, the record of daily mean flow shows that discharge in excess of 10 cms is not common, especially for certain seasons in the spring and summer months. For example, flow above 10 cms occurs in June or July in only 1 out of every 10 years statistically (Figure 17). For the snowmelt runoff period of March and April it is more probable this threshold will be exceeded, but the chance is still only 50% (Figure 17). Because the life history cycles of many organisms rely on habitat at specific times of the year to survive, it is important to consider these seasonal patterns of streamflow.

The protected backwater habitat in this channel at flows below 10 cms is also an important element of the stream geometry because it has lower mean flow velocities and depths than the main channel. Such areas enhance ecosystem function by providing sites for primary production of algae, growth of aquatic stage invertebrates, and refugia for young fishes. Another important quality of this channel that is confirmed by the hydraulic model results is that it is dynamic because its longitudinal profile allows it to accept inflow from upstream when discharge rises above 10 cms. When water flows through this area, the physical, chemical, and biological

processes will proceed differently than if it were functioning only as a backwater. For example, the export of organic matter will be low for this area when it is in non-flowing backwater status, but as discharge increases above 10 cms export rates climb as material is returned to the main channel. Similar changes in temperature and water chemistry regimes will occur as the channel transitions between states. This variability increases spatial and temporal heterogeneity in the floodplain, and addresses recommendations in the scientific literature for river restoration efforts to be attentive to reestablishing natural process (Wohl *et al.*, 2005) and habitat mosaics (Hauer *et al.*, 2003).

Signs of enhanced floodplain connectivity with the restoration are seen in the hydraulic model results for the existing parafluvial zone on the left bank as well (Figure 15). As discharge increases, flooding here continues to occur much like it does with the existing stream geometry, but with a slightly diminished area of inundation. The simulation results indicate that this is possible because as the existing parafluvial zone receives progressively more overbank flow at higher discharge, the water surface area in the new overflow channel increases only slightly. This is important because it maintains the process of flooding in the existing parafluvial zone rather than sacrificing it by allowing all the overbank flow to be directed into the restored area. This balance is achieved by assigning elevations to the longitudinal profile of the overflow channel that insure the parafluvial zone is inundated at a slightly lower discharge than the discharge that causes the overflow channel to begin flowing (Figure 15A). The end result of creating new lateral connections to the channel while still maintaining existing connections is an increase in the maximum flooded width of the floodplain at all levels of discharge (Figure 16). This augments the size of the unique and valuable riparian ecotone.

The objectives and general approach of this study can be appreciated in the context of other restoration efforts in the U.S. Southwest following the analysis by Follstad Shah and others (2007) of 576 stream restoration projects implemented in this region since 1990. The restoration plan in the current study with its dual objectives of channel reconfiguration and floodplain reconnection has the same intent of only 10% of the studies in this comprehensive analysis. The reach length of the current study would be categorized as “less than or equal to 3 km”, which matches 50% of the 576 projects. The current effort can be distinguished from the vast majority of the restoration activities evaluated for the U.S. Southwest because it has good potential for post-implementation monitoring, which was associated with only 28% of the undertakings examined from this region. Specifically, the current project’s combination of well-defined objectives, hydraulic simulations, and quality elevation data would expedite designing a monitoring program and evaluating results.

The methods and hydrologic processes that are central to the current project are also relevant to questions not directly related to restoration. For example, a recent study of streams in the same Gila basin of southwestern New Mexico found that phosphate, which is associated with sediment in stream channels, increases in concentration with discharge (Acuña and Dahm, 2007). One conceivable way to better understand the sources of phosphate in this stream network that would follow the example of the current study would be to build a hydraulic model with results mapped in a GIS in order to predict the total area of inundation upstream of a sample site. In this way it may be possible to explain phosphate concentrations better than by using only the magnitude of discharge.

The modeling platform used in the current study could also be adapted to help water managers and planners address other issues. Planning for effects of recently documented meteorological trends in the western U.S. such as more precipitation falling as rain rather than snow (Knowles *et al.*, 2006) could be done by making season-specific adjustments to the past record. The current approach would be useful for such applications because it explicitly considers hydrologic characteristics such as water volume, flooded area, and daily mean flow records. It also has flexibility suitable for such uses because hydrologic input and elevation data can be modified quickly to accommodate alternative scenarios. In order to take full advantage of these tools, however, investment in public resources such as high-resolution elevation data and improved hydrological monitoring is required.

## CONCLUSIONS

This case study demonstrates the need for stream restoration, designs the restoration plan, and evaluates the merits of the plan using a physically-based model. The need for restoration is appreciated first by field visits, in which signs of past agricultural activity, a disconnected floodplain, and a riparian zone lacking riparian vegetation can be appreciated as signs of past channelization. Research is done to confirm this past activity, which is verified through documents and photographs created by the USGS and available from the agency upon request. To design a robust restoration plan that can be evaluated for improved habitat, the site is surveyed using LIDAR and by physical measurements across the channel. LIDAR-surveyed points that represent vegetation are removed from the data, the LIDAR point cloud is georeferenced using targets registered in the LIDAR data and described using a GPS, and the

dataset is brought into a GIS where the in-channel measurements are added for bathymetry to complete the surface model of the site. A copy of the surface model is modified to make a second model that represents the restoration design, incorporating an overflow channel to provide more aquatic habitat and increase floodplain connectivity with the main channel. Steady flow 1-D hydraulic models of open channel flow are created using each surface model and a range of expected flows.

The hydraulic models work well, and their results are compared in a GIS, illustrating clear differences between the existing configuration and the restored configuration. The primary differences are that the restored plan has more flooded area at each level of discharge, and that the new channel provides valuable backwater habitat. The most relevant discharges to consider from the wide range of flows used in the models are chosen based on which are likely to occur during each distinct flow period. The maximum difference in flooded area between the two configurations is about 11%, while the maximum difference in total volume is 7%. In addition, the maximum width of the flooded extent of the riparian area is greater with the restored configuration. The portion of the existing floodplain that currently floods at moderately high flows still does so, but it is slightly attenuated in extent. The restoration design provides more habitat at flow levels that occur at the site, and floodplain connectivity and heterogeneity increase as a result of the restored configuration.

## REFERENCES

- Aarts BGW, Van den Brink FWB, Nienhuis PH. 2004. Habitat loss as the main cause of the slow recovery of fish faunas of regulated large rivers in Europe: the transversal floodplain gradient. *River Research and Applications* **20**: 3–23. DOI: 10.1002/rra.720.
- Acuña V, Dahm CN. 2007. Impact of monsoonal rains on spatial scaling patterns in water chemistry of a semiarid river network. *Journal of Geophysical Research* 112: G04009, 11 pp. DOI:10.1029/2007JG000493.
- Axelsson P. 2000. DEM generation from laser scanner data using adaptive TIN models. *International Archives of Photogrammetry and Remote Sensing* **33**: 110-117.
- Barnes HH. 1967. *Roughness Characteristics of Natural Channels*. Water-Supply Paper 1849. U.S. Geological Survey: Reston, VA; 213 pp.
- Bayley PB. 1995. Ecology of large rivers. *Bioscience* **45**: 153-158.
- Bernhardt ES, Palmer MA, Allan JD, Alexander G, Barnas K, Brooks S, Carr J, Clayton S, Dahm C, Follstad-Shah J, Galat D, Gloss S, Goodwin P, Hart D, Hassett B, Jenkinson R, Katz S, Kondolf GM, Lake PS, Lave R, Meyer JL, O'Donnell TK, Pagano L, Powell B, Sudduth E. 2005. Synthesizing U.S. river restoration efforts. *Science* **308**: 636-637. DOI: 10.1126/science.1109769.

- Blodgett DD. 1973. *Hydrogeology of the San Augustin Plains, New Mexico*. Unpublished M.S. Thesis. New Mexico Institute of Mining and Technology: Socorro, NM; 55 pp.
- Bovee KD, Lamb BL, Bartholow JM, Stalnaker CB, Taylor J, Henriksen J. 1998. *Stream Habitat Analysis Using the Instream Flow Incremental Methodology*. Information and Technology Report USGS/BRD 1998-0004. U.S. Geological Survey: Reston, VA; 131 pp. <http://www.fort.usgs.gov/Products/Publications/3910/3910.pdf> [accessed 5 October 2010].
- Brookes A, Gregory KJ, Dawson FH. 1983. An assessment of river channelization in England and Wales. *The Science of the Total Environment* **27**: 97-111.
- Brookes A. 1988. *Channelized Rivers: Perspectives for Environmental Management*. Wiley: Chichester, UK; 326 pp.
- Brown TC, Bergstrom JC, Loomis JB. 2007. Defining, valuing, and providing ecosystem goods and services. *Natural Resources Journal* **47**: 329-376.
- Bryan K. 1928. Change in plant associations by change in ground water level. *Ecology* **9**: 474-478.
- Chow VT. 1959. *Open-channel Hydraulics*. McGraw-Hill: New York; 700 pp.
- Coates DR. 1981. *Environmental Geology*. Wiley: New York; 701 pp.

Costanza R, d'Arge R, de Groot R, Farber S, Grasso M, Hannon B, Limburg K, Naeem S, O'Neill RV, Paruelo J, Raskin RG, Sutton P, van den Belt M. The value of the world's ecosystem services and natural capital. *Nature* **387**: 253-260.

Daily, GC. 1997. Introduction: what are ecosystem services? In *Nature's Services: Societal Dependence on Natural Ecosystems*. Daily GC (ed). Island Press: Washington, DC; 1-10.

de Groot RS, Wilson MA, Boumans RMJ. 2002. A typology for the classification, description and valuation of ecosystem functions, goods and services. *Ecological Economics* **41**: 393-408.

Dunn CN, Hickey JT. 2003. The Ecosystem Functions Model (EFM): A tool for restoration planning. *World Water Congress (ASCE Conf. Proc.)* **118**: 327-338. DOI: 10.1061/40685(2003)327.

ESRI. 2010a. *ArcMap GIS*. <http://www.esri.com>.

ESRI. 2010b. *ArcScene GIS*. <http://www.esri.com>.

European Commission. 2000: Directive 2000/60/EC of the European Parliament and of the Council establishing a framework for Community action in the field of water policy (EU Water Framework Directive). Official Journal L 327; 12 December 2000. <http://eur->

lex.europa.eu/LexUriServ/LexUriServ.do?uri=OJ:L:2000:327:0001:0072:EN:PDF [accessed 15 June 2011].

Fleck J. 2011. High & Dry. *Albuquerque Journal* 3 April 2011. Albuquerque Publishing Company: Albuquerque, NM.

Follstad Shah JJ, Dahm CN, Gloss SP, Bernhardt ES. 2007. River and riparian restoration in the Southwest: results of the National River Restoration Science Synthesis Project. *Restoration Ecology* **15**: 550-562. DOI: 10.1111/j.1526-100X.2007.00250.x.

Galat DL, Fredrickson LH, Humburg DD, Bataille KJ, Bodie JR, Dohrenwend J, Gelwicks GT, Havel JE, Helmers DL, Hooker JB, Jones JR, Knowlton MF, Kubisiak J, Mazourek J, McColpin AC, Renken RB, Semlitsch RD. 1998. Flooding to restore connectivity of regulated, large-river wetlands. *BioScience* **48**: 721-733.

Galay VJ. 1983. Causes of river bed degradation. *Water Resources Research* **19**: 1057-1090.

Gergel SE, Carpenter SR, Stanley EH. 2005. Do dams and levees impact nitrogen cycling? Simulating the effects of flood alterations on floodplain denitrification. *Global Change Biology* **11**: 1352-1367. DOI: 10.1111/j.1365-2486.2005.00966.x.

Graf WL. 2001. Damage control: Restoring the physical integrity of America's rivers. *Annals of the Association of American Geographers* **91**: 1-27.

Gregory SV, Swanson FJ, McKee WA, Cummins KW. 1991. An ecosystem perspective of riparian zones. *Bioscience* **41**: 540-551.

Grubaugh JW, Anderson RV. 1988. Spatial and temporal availability of floodplain habitat: long-term changes at Pool 19, Mississippi River. *American Midland Naturalist* **119**: 402-411.

Harvey MD, Watson CC. 1986. Fluvial processes and morphological thresholds in incised channel restoration. *Water Resources Bulletin* **22**: 359–368.

Hauer FR, Dahm CN, Lamberti GA, Stanford JA. 2003. Landscapes and ecological variability of rivers in North America: Factors affecting restoration strategies. In *Strategies for Restoring River Ecosystems: Sources of Variability and Uncertainty in Natural and Managed Systems*. Wissmar RC, Bisson PA (eds). American Fisheries Society: Bethesda, MD; 81-105.

Hesselink AW, Weerts HJT, Berendsen HJA. 2003. Alluvial architecture of the human-influenced river Rhine, The Netherlands. *Sedimentary Geology* **161**: 229-248.

InnovMetric Software Inc. 2008a. *PolyWorks/IMAlign™ 3D Image Alignment Software Reference Guide Version 10.1 for Windows*. InnovMetric Software: Quebec.

InnovMetric Software Inc. 2008b. *PolyWorks/IMInspect™ Comparison and Verification Software Reference Guide Version 10.1 for Windows*. InnovMetric Software: Quebec.

- Jähnig SC, Lorenz A, Hering D. 2008. Hydromorphological parameters indicating differences between single- and multiple-channel mountain rivers in Germany, in relation to their modification and recovery. *Aquatic Conservation: Marine and Freshwater Ecosystems* **18**: 1200-1216. DOI: 10.1002 / aqc.875.
- Jones JL. 2006. Side channel mapping and fish habitat suitability analysis using lidar topography and orthophotography. *Photogrammetric Engineering & Remote Sensing* **72**: 1202-1206.
- Junk WJ, Bayley PB, Sparks RE. 1989. The flood pulse concept in river-floodplain systems. *Canadian Special Publication Fisheries and Aquatic Sciences* **106**: 110-127.
- Kingsford RT. 2000. Ecological impacts of dams, water diversions and river management on floodplain wetlands in Australia. *Austral Ecology* **25**: 109-127.
- Knighton D. 1998. *Fluvial Forms and Processes*. Oxford Univ. Press: New York; 383 pp.
- Knippertz P, Martin JE. 2007. A Pacific Moisture Conveyor Belt and its relationship to a significant precipitation event in the semiarid Southwestern United States. *Weather and Forecasting* **22**:125-144. DOI: 10.1175/WAF963.1.
- Knowles N, Dettinger MD, Cayan DR. 2006. Trends in snowfall versus rainfall in the western United States. *Journal of Climate* **19**: 4545-4559. DOI: 10.1175/JCLI3850.1.

- Kondolf GM, Boulton AJ, O'Daniel S, Poole GC, Rahel FJ, Stanley EH, Wohl E, Bång A, Carlstrom J, Cristoni C, Huber H, Koljonen S, Louhi P, Nakamura K. 2006. Process-based ecological river restoration: visualizing three-dimensional connectivity and dynamic vectors to recover lost linkages. *Ecology and Society* **11** [Internet]. <http://www.ecologyandsociety.org/vol11/iss2/art5/> [accessed 15 June 2011].
- Laeser SR, Baxter CV, Fausch KD. 2005. Riparian vegetation loss, stream channelization, and web-weaving spiders in northern Japan. *Ecological Research* **20**: 646–651. DOI: 10.1007/s11284-005-0084-3.
- Lair G, Zehetner F, Fiebig M, Gerzabek MH, van Gestel CAM, Hein T, Hohensinner S, Hsu P, Jones KC, Jordan G, Koelmans AA, Poot A, Slijkerman DME, Totsche KU, Bondar-Kunze E, Barth JAC. 2009. How do long-term development and periodical changes of river-floodplain systems affect the fate of contaminants? Results from European rivers. *Environmental Pollution* **157**: 3336–3346. DOI: 10.1016/j.envpol.2009.06.004.
- Lefsky MA, Cohen WB, Parker GG, Harding DJ. 2002. Lidar remote sensing for ecosystem studies. *Bioscience* **52**: 19-30.
- Lepori F, Palm D, Malmqvist B. 2005. Effects of stream restoration on ecosystem functioning: detritus retentiveness and decomposition. *Journal of Applied Ecology* **42**: 228–238. DOI: 10.1111/j.1365-2664.2004.00965.x.

Limerinos JT. 1970. *Determination of the Manning Coefficient from Measured Bed Roughness in Natural Channels*. Water-Supply Paper 1898-B. U.S. Geological Survey: Reston, VA; 47 pp.

Lloyd N, Quinn G, Thoms M, Arthington A, Gawne B, Humphries P, Walker K. 2003. *Does Flow Modification Cause Geomorphological and Ecological Response in Rivers? A Literature Review from an Australian Perspective*. Technical report 1/200. Cooperative Research Centre for Freshwater Ecology: Canberra; 51 pp. <http://freshwater.canberra.edu.au/publications.nsf> [accessed 16 June 2011].

Lytle DA, Poff NL. 2004. Adaptation to natural flow regimes. *Trends in Ecology & Evolution* **19**: 94-100. DOI: 10.1016/j.tree.2003.10.002.

Maddock I. 1999. The importance of physical habitat assessment for evaluating river health. *Freshwater Biology* **41**: 373-391.

McKean JA, Isaak DJ, Wright CW. 2008. Geomorphic controls on salmon nesting patterns described by a new, narrow-beam terrestrial-aquatic lidar. *Frontiers in Ecology and the Environment* **6**: 125-130. DOI: 10.1890/070109.

Mertes LAK. 2002. Remote sensing of riverine landscapes. *Freshwater Biology* **47**: 799-816.

- Merwade V, Cook A, Coonrod J. 2008a. GIS techniques for creating river terrain models for hydrodynamic modeling and flood inundation mapping. *Environmental Modelling & Software* **23**: 1300-1311.
- Merwade V. 2008b. Creating river bathymetry mesh from cross-sections. [http://web.ics.purdue.edu/~vmerwade/research/terrain\\_tutorial.pdf](http://web.ics.purdue.edu/~vmerwade/research/terrain_tutorial.pdf). [accessed 21 April 2010].
- Mussetter Engineering Inc. (MEI). 2006. *Geomorphology of the Upper Gila River within the State of New Mexico*. MEI Project No. 05-23, submitted to New Mexico Interstate Stream Commission; 241 pp. <http://www.ose.state.nm.us/PDF/ISC/BasinsPrograms/GilaSanFrancisco/Mussetter-2006-Geomorphology-UpperGila.pdf> [accessed 16 June 2011].
- Myers RG, Everheart JT, Wilson CA. 1994. *Geohydrology of the San Agustin Basin, Alamosa Creek Basin upstream from Monticello Box, and upper Gila Basin in parts of Catron, Socorro, and Sierra Counties, New Mexico*. Water Resources Investigations Report 94-4125. U.S. Geological Survey: Reston, VA; 70, pp.
- Naiman RJ, Décamps H. 1997. The ecology of interfaces: riparian zones. *Annual Review of Ecology and Systematics* **28**: 621-658.

- Nakano D, Nakamura F. 2006. Responses of macroinvertebrate communities to river restoration in a channelized segment of the Shibetsu River, northern Japan. *River Research and Applications* **22**: 681-689.
- Nakano D, Nakamura F. 2008. The significance of meandering channel morphology on the diversity and abundance of macroinvertebrates in a lowland river in Japan. *Aquatic Conservation: Marine and Freshwater Ecosystems* **18**: 780–798. DOI: 10.1002/aqc.885.
- National Geodetic Survey. 2010. NGS Geodetic Tool Kit. <http://www.ngs.noaa.gov/TOOLS/> [accessed 19 April 2010].
- New Mexico Environmental Law Center. 2011. Augustin Plains Ranch water rights application. [http://nmenvirolaw.org/index.php/site/cases/san\\_augustin\\_plains\\_ranch\\_water\\_rights\\_application/](http://nmenvirolaw.org/index.php/site/cases/san_augustin_plains_ranch_water_rights_application/) [accessed 11 June 2011].
- New Mexico Interstate Stream Commission (NMISC). 2006. *Briefing on Upper Gila River Settlement Decision Process*; 25 pp. <http://www.ose.state.nm.us/PDF/ISC/BasinsPrograms/GilaSanFrancisco/BriefingPacket-7-3-2006.pdf> [accessed 11 June 2011].
- Olden JD, Poff NL. 2003. Redundancy and the choice of hydrologic indices for characterizing streamflow regimes. *River Research and Applications* **19**: 101-121.

Olivier JM, Carrel G, Lamouroux N, Dole-Olivier MJ, Malard F, Bravard JP, Amoros C. 2009. The Rhône River Basin. In *Rivers of Europe*. Tockner K, Uehlinger U, Robinson CT (eds). Elsevier/Academic Press: San Diego, CA; 247-295.

Opperman JJ, Galloway GE, Fargione J, Mount JF, Richter BD, Secchi S. 2009. Sustainable floodplains through large-scale reconnection to rivers. *Science* **326**: 1487-1488.

Opperman JJ, Luster R, McKenney BA, Roberts M, Meadows AW. 2010. Ecologically functional floodplains: Connectivity, flow regime, and scale. *Journal of the American Water Resources Association* **46**: 211-226. DOI: 10.1111/j.1752-1688.2010.00426.x.

Optech Inc. 2006. *ILRIS-3D Operation Manual 0040170/Revision A*. Optech Technical Publications: Vaughan, Ontario.

Overton IC. 2005. Modelling floodplain inundation on a regulated river: integrating GIS, remote sensing and hydrological models. *River Research and Applications* **21**: 991-1001. DOI: 10.1002/rra.867.

Petts GE. 2009. Instream flow science for sustainable river management. *Journal of the American Water Resources Association* **45**: 1071-1086. DOI: 10.1111/j.1752-1688.2009.00360.x.

- Poff NL, Allan JD, Bain MB, Karr JR, Presteggaard KL, Richter BD, Sparks RE, Stromberg JC. 1997. The natural flow regime: A paradigm for river conservation and restoration. *Bioscience* **47**: 769-784.
- Pollock MM, Naiman RJ, Hanley TA. 1998. Plant species richness in riparian wetlands—a test of biodiversity theory. *Ecology* **79**: 94-105.
- Powell SJ, Letcher RA, Croke BFW. 2008. Modelling floodplain inundation for environmental flows: Gwydir wetlands, Australia. *Ecological Modelling* **211**: 350-362. DOI: 10.1016/j.ecolmodel.2007.09.013.
- Reid HE, Gregory CE, Brierley GJ. 2008. Measures of physical heterogeneity in appraisal of geomorphic river condition for urban streams: Twin Streams catchment, Auckland, New Zealand. *Physical Geography* **29**: 247-274.
- Richards K, Brasington J, Hughes F. 2002. Geomorphic dynamics of floodplains: ecological implications and a potential modelling strategy. *Freshwater Biology* **47**: 559–579.
- Sheibley RW, Ahearn DS, Dahlgren RA. 2006. Nitrate loss from a restored floodplain in the Lower Cosumnes River, California. *Hydrobiologia* **571**: 261–272. DOI: 10.1007/s10750-006-0249-2.

- Simon, A. 1989. A model of channel response in disturbed alluvial channels. *Earth Surface Processes and Landforms* **14**: 11–26.
- Soles, ES. 2003. *Where the River Meets the Ditch: Human and Natural Impacts on the Gila River, New Mexico, 1880-2000*. M.A. Thesis. Northern Arizona University: Flagstaff; 166 pp.
- Strickler A. 1923. Beitrage zur Frage der Geschwindigkeitsformel und der Rauigkeitszahlen fur Strome, Kanale und geschlossene Leitungen. (Contributions to the formula of flow velocity and to the estimation of flow resistance for rivers, channels and closed conduits). Mitteilung Nr. 16 des Amtes für Wasserwirtschaft; Eidg. Departement des Inneren, Bern.
- Stromberg JC, Tiller R, Richter B. 1996. Effects of groundwater decline on riparian vegetation of semiarid regions: The San Pedro, Arizona. *Ecological Applications* **6**: 113-131.
- Sturm TW. 2001. *Open Channel Hydraulics*. McGraw-Hill: New York; 493 pp.
- Tockner K, Stanford JA. 2002. Riverine flood plains: present state and future trends. *Environmental Conservation* **29**: 308–330. DOI:10.1017/S037689290200022X.
- Terrasolid Ltd. 2010a. *TerraScan User's Guide*. Terrasolid: Jyväskylä, Finland.  
[http://www.terrasolid.fi/system/files/tscan\\_1.pdf](http://www.terrasolid.fi/system/files/tscan_1.pdf). [accessed 21 April 2010].

Terrasolid Ltd. 2010b. *TerraScan brochure*. Terrasolid: Jyväskylä, Finland.

[http://www.terrasolid.fi/system/files/TerraScan\\_eng\\_2.pdf](http://www.terrasolid.fi/system/files/TerraScan_eng_2.pdf). [accessed 21 April 2010].

Thoms MC. 2003. Floodplain-river ecosystems: lateral connections and the implications of human interference. *Geomorphology* **56**: 335-349.

Trimble. 2009. *GPS Pathfinder ProXH Receiver Datasheet*. [http://trl.trimble.com/docushare/dsweb/Get/Document-219806/022501-022I\\_GPS%20Pathfinder%20ProXH\\_DS\\_1209\\_LR.pdf](http://trl.trimble.com/docushare/dsweb/Get/Document-219806/022501-022I_GPS%20Pathfinder%20ProXH_DS_1209_LR.pdf). [accessed 21 April 2010].

United States (US). 2005. New Mexico Consumptive Use and Forbearance Agreement.

<http://www.ose.state.nm.us/PDF/ISC/BasinsPrograms/GilaSanFrancisco/Final-CUFA-Oct27-2005.pdf>. [accessed 11 June 2011].

U.S. Army Corps of Engineers (USACE). 2010. *HEC-RAS River Analysis System,*

*User's manual Version 4.1*. Hydrologic Engineering Center: Davis, CA.

U.S. Army Corps of Engineers (USACE). 2009a. *HEC-EFM Ecosystem Functions Model*

*Quick Start Guide Version 2.0*. Hydrologic Engineering Center: Davis, CA.

U.S. Army Corps of Engineers (USACE). 2009b. *HEC-GeoRAS: GIS tools for support of*

*HEC-RAS using ArcGIS, User's manual Version 4.2*. Hydrologic Engineering Center: Davis, CA.

U.S. Geological Survey (USGS). 1930-1960. Discharge Measurement Notes (form 9-275c) Gila River near Gila, NM. Unpublished data.

U.S. Geological Survey (USGS). 2010a. Water-Data Report 2008, 09430500 Gila River near Gila, NM. <http://wdr.water.usgs.gov/wy2008/pdfs/09430500.2008.pdf> [accessed April 10, 2010].

U.S. Geological Survey (USGS). 2010b. National Water Information System: Web Interface, USGS 09430500 Gila River near Gila, NM. [http://waterdata.usgs.gov/nm/nwis/uv/?site\\_no=09430500&PARAMeter\\_cd=00065,00060](http://waterdata.usgs.gov/nm/nwis/uv/?site_no=09430500&PARAMeter_cd=00065,00060) [accessed 29 January 2011].

U.S. Geological Survey (USGS). 2010c. Station Description, 09430500 Gila River near Gila, NM. Available electronically in the USGS Station Information Management System. Unpublished data.

Van Urk G, Smit H. 1989. The Lower Rhine: Geomorphological changes. In *Historical Change of Large Alluvial Rivers: Western Europe*. Petts GE, Möller H, Roux AL (eds). Wiley: Chichester, UK; 167-182.

Vierling KT, Vierling LA, Gould WA, Martinuzzi S, Clawges RM. 2008. Lidar: shedding new light on habitat characterization and modeling. *Frontiers in Ecology and the Environment* 6: 90-98. DOI: 10.1890/070001.

- Vierling LA, Martinuzzi S, Asner GP, Stoder J, Johnson BR. 2011. LiDAR: providing structure. *Frontiers in Ecology and the Environment* **9**: 261-262. DOI: 10.1890/11.WB.009.
- Ward JV, Stanford JA. 1995. The serial discontinuity concept: extending the model to floodplain rivers. *Regulated Rivers: Research & Management* **10**: 159-168.
- Ward JV, Tockner K, Arscott DB, Claret C. 2002. Riverine landscape diversity. *Freshwater Biology* **47**: 517-539.
- Ward JV, Tockner K, Uehlinger U, Malard F. 2001. Understanding natural patterns and processes in river corridors as the basis for effective river restoration. *Regulated Rivers: Research & Management* **17**: 311-323.
- Williams PB, Andrews E, Opperman JJ, Bozkurt S, Moyle PB. 2009. Quantifying activated floodplains on a lowland regulated river: its application to floodplain restoration in the Sacramento Valley. *San Francisco Estuary and Watershed Science* [Internet]. 1-25. <http://repositories.cdlib.org/jmie/sfews/vol7/iss1/art4>.
- Wohl E. 2005. Compromised rivers: Understanding historical human impacts on rivers in the context of restoration. *Ecology and Society* **10**: 24-40.

Wohl E, Angermeier PL, Bledsoe B, Kondolf GM, MacDonnell L, Merritt DM, Palmer MA, Poff NL, Tarboton D. 2005. River restoration. *Water Resources Research* **41**: W10301. DOI: 10.1029/2005WR003985.

Xu J. 1993. A study of long term environmental effects of river regulation on the Yellow River of China in historical perspective. *Geografiska Annaler. Series A, Physical Geography* **75**: 61-72.

## APPENDIX

*Appendix 1.* Stream discharge levels modeled with HEC-RAS in units of cubic meters per second (cms) and cubic feet per second (cfs).

cms	cfs	cms	cfs
1	35	60	2119
2	71	70	2472
3	106	80	2825
4	141	90	3178
5	177	100	3531
6	212	110	3884
7	247	120	4237
8	282	130	4590
9	318	140	4943
10	353	150	5297
11	388	200	7062
12	424	250	8828
13	459	300	10593
14	494	400	14124
16	565	500	17655
18	636	600	21186
20	706	700	24717
30	1059	800	28248
40	1412	900	31779
50	1766	1000	35310